Prog. Biophys. molec. Biol., Vol. 53, pp. 1–31, 1989.
Printed in Great Britain.

0079-6107/89 $0.00+.50

THE FOURIER APPROACH TO THE IDENTIFICATION OF FUNCTIONAL COUPLING BETWEEN NEURONAL SPIKE TRAINS

J. R. ROSENBERG*, A. M. AMJAD†, P. BREEZE†, D. R. BRILLINGER‡ and D. M. HALLIDAY*

Departments of Physiology and Statistics†, University of Glasgow, Scotland and Department of Statistics‡, University of California, Berkeley, U.S.A.*

CONTENTS

I. INTRODUCTION

The study of the behaviour of small networks of neurones frequently requires the determination of measures of the strength of association between component neurones, an assessment of their timing relations, and the identification of which neurones may interact directly or are influenced by common inputs.

In many of these studies the principal quantities available for analysis are the sequences of extracellularly recorded action potentials (neuronal spike trains). The subsequent analytical work is then based entirely on the relations between the times of occurrence of the action potentials recorded from different neurones. In these circumstances neuronal spike trains are frequently represented as the mathematical entity known as a stochastic point process. These processes are described by providing a probability law for a set of ordered times

$$\cdots < \tau_{-2} < \tau_{-1} < \tau_0 < \tau_1 < \tau_2 < \cdots,$$

to be thought of as the realized times of occurrence of the action potentials in a spike train. In many respects point processes are like ordinary time series, that is, the usual signals that occur in many dynamic analyses. There are, however, mathematically subtle differences between point processes and ordinary time series that must be taken into account when setting down definitions and in providing analysis techniques. Pertinent references to the point process literature include Cox and Isham (1980), Cox and Lewis (1968), Cox and Lewis

Address for correspondence: J. R. Rosenberg, Department of Physiology, University of Glasgow, Glasgow G12 8QQ, Scotland.

(1972), Daley and Vere-Jones (1988), and Lewis (1972a,b), whereas a comparison of ordinary time series and point processes may be found in Brillinger (1978).

There are several approaches to measures of association between spike trains. Following on from the early work of Gerstein and Kiang (1960) and Griffith and Horn (1963) are those procedures based on cross-correlation methods, or functions derived from them, such as the CUSUM or the ratio of the peak of the estimated cross-intensity to its baseline. Examples of this approach, applied to a variety of preparations, may be found in Bryant *et al.* (1973), Ellaway and Murthy (1985a,b), Kirkwood and Sears (1982) and Toyama *et al.* (1981), and were originally reviewed by Moore *et al.* (1966), discussed extensively by Perkel *et al.* (1967a,b), and more recently reviewed by Kirkwood (1979) and Kirkwood and Sears (1980) with special reference to the mammalian central nervous system; further assessed by Aertsen and Gerstein (1985) and more recently extended by Melssen and Epping (1987), where additional references may also be found.

Cox and Lewis (1972) and Lewis (1972a) indicate some of the difficulties, from a statistical point of view, of the above approach to measures of association between spike trains. Brillinger (1986) has also discussed the disadvantage of a cross-correlation based approach to measures of association, and has also pointed out that the cross-intensity function used as the basis for these time-domain measures of association is the point-process analogue of covariance, and consequently may be expected to have the same limitations. The disadvantages of the use of covariance as a measure of association are widely known and may be summarized as follows: (1) it is dimensional, its value depends on the units of measurement, and (2) it is not bounded, which means that although a zero covariance indicates the absence of a linear relationship, there is no value indicating a perfect linear relationship.

Given the limitations of covariance-based measures of association in many situations, one usually turns to a regression type of analysis (Brillinger, 1986; Brillinger and Tukey, 1984), which in the frequency-domain leads naturally to measures of association based on the Fourier transforms of the processes (Brillinger, 1986). Regression analysis is associated with correlation rather than covariance, and the correlation coefficient has the advantages that it is both dimensionless and normative—zero indicating a lack of a linear relationship and the values ± 1 indicating a perfect linear relationship. All the values of the correlation coefficient necessarily lie between -1 and $+1$, and its square can be interpreted as a measure of how well the linear regression accounts for the relation between two variables. One frequency-domain measure of association, analogous to correlation-squared, called the coherence, provides a normative measure of the strength of association on a scale from zero to one, with zero occurring in the case of independence and corresponding to the absence of a linear time-invariant relationship. Although there are some examples of coherence applied to model generated data (Stein *et al.*, 1972) and illustrations of its applications in a system identification context (Brillinger, 1975a; Brillinger *et al.*, 1976), or in relation to some aspects of motor control (e.g. Clark *et al.*, 1981; Houk *et al.*, 1987), the wide range of usefulness of the coherence for point processes seems in need of more exploration together with several related frequency-domain measures of association that have not been developed and discussed in relation to spike train analysis.

The object of the present report, therefore, is firstly to provide an extensive development and description of the wide range of applicability of a Fourier approach to measures of association and related problems, and secondly, to compare time- and frequency-domain measures of association between spike trains with respect to different representations of features of a data set. Of particular interest is the question of whether the association between a pair of neurones is a consequence of a common input or of a direct connection, and the extended question of how the relation between a pair of neurones—their strength of association and relative timing—is influenced by the presence of several other inputs. We have selected examples which illustrate how some frequency-domain parameters provide alternatives to time-domain measures of association and allow one to set up simple statistical tests for comparing the difference in the strength of association between pairs of spike trains and for detecting synchronous activity. Frequency-domain measures of association between

spike trains are also shown to be easily applied to the analysis of interactions between several spike trains in a manner not possible by conventional time-domain methods.

Preliminary studies of some of these problems have been presented elsewhere (Amjad *et al.*, 1988; Rosenberg and Rigas, 1985).

II. NOTATION AND STOCHASTIC POINT PROCESS PARAMETERS

A realization or a sample of a point process may be represented by a counting measure, denoted as

$$N(t)=\#\{\tau_j, 0<\tau_j\leq t\} \tag{2.1}$$

where $\#\{\ \}$ indicates the number of events in the interval $(0, t]$ and $\{\tau_j\}$ the set of spike times in the sample. In defining point-process parameters it is convenient to introduce differential increments of the process N defined as

$$\mathrm{d}N(t)=N(t, t+\mathrm{d}t] \tag{2.2}$$

and giving the number of events in a small interval $(t, t+\mathrm{d}t]$ of duration $\mathrm{d}t$.

It will be assumed (a) that the points of the process N do not occur simultaneously (the process is orderly), (b) the parameters characterizing the process do not change with time (the process is stationary), and (c) the number of events occurring in intervals widely separated in time are essentially independent (the process is mixing). A full discussion of these assumptions may be found in Cox and Isham (1980), Cox and Lewis (1972) and Daley and Vere-Jones (1988).

The mean intensity of the process N is defined as

$$P_N=\lim_{h\to 0}\mathrm{Prob}\{N \text{ event in } (t, t+h]\}/h \tag{2.3}$$

and since the process is orderly P_N may be interpreted via the relationship

$$E\{\mathrm{d}N(t)\}=P_N\,\mathrm{d}t \tag{2.4}$$

where $E\{\ \}$ denotes the averaging operator or mathematical expectation of a random variable.

In the case that one has a bivariate point process, $[M(t), N(t)]$, the second-order cross-product density at lag u, $P_{NM}(u)$, is defined as

$$P_{NM}(u)=\lim_{h,h'\to 0}\mathrm{Prob}\{N \text{ event in } (t+u, t+u+h] \quad \text{and} \quad M \text{ event in } (t, t+h']\}/hh' \tag{2.5}$$

and may be interpreted through the relation

$$E\{\mathrm{d}N(t+u)\,\mathrm{d}M(t)\}=P_{NM}(u)\,\mathrm{d}u\,\mathrm{d}t. \tag{2.6}$$

A conditional mean intensity is defined as

$$m_{NM}(u)=\frac{P_{NM}(u)}{P_M} \tag{2.7}$$

and may be interpreted as

$$m_{NM}(u)=\lim_{h\to 0}\mathrm{Prob}\{N \text{ event in } (t+u, t+u+h] \quad \text{given an } M \text{ event at } t\}/h \tag{2.8}$$

or in terms of expected values as

$$E\{\mathrm{d}N(t+u)/M \text{ event at time } t\}=\frac{P_{NM}(u)\,\mathrm{d}u}{P_M}. \tag{2.9}$$

In the case that $u \neq 0$ the product density and conditional intensity may be obtained for each process alone from (2.5) and (2.7) by setting M equal to N. The value of $P_{NN}(u)$ at $u=0$ is defined to make the function continuous at that point.

For many processes of interest, specifically those that are mixing, as u becomes large, increments of the process become independent, for example

$$\lim_{|u|\to\infty} P_{NM}(u) = P_N P_M. \tag{2.10}$$

This phenomenon leads to the definition of cross-covariance density as

$$q_{NM}(u) = P_{NM}(u) - P_N P_M \tag{2.11a}$$

which tends to zero as $|u|\to\infty$, and has the interpretation.

$$\operatorname{cov}\{dN(t+u),\, dM(t)\} = q_{NM}(u)\, du\, dt, \tag{2.11b}$$

where "cov" denotes covariance.

Following Bartlett (1963), the cross-spectrum between two point-processes at frequency λ, $f_{NM}(\lambda)$, is defined as

$$f_{NM}(\lambda) = \frac{1}{2\pi}\int_{-\infty}^{\infty} q_{NM}(u) e^{-i\lambda u}\, du \tag{2.12}$$

whereas in the case of a single process, the auto-spectrum, $f_{NN}(\lambda)$, is defined as

$$f_{NN}(\lambda) = \frac{P_N}{2\pi} + \frac{1}{2\pi}\int_{-\infty}^{\infty} q_{NN}(u) e^{-i\lambda u}\, du. \tag{2.13}$$

The additional term in (2.13) corresponds to the inclusion of $\delta(u)$, the Dirac δ-function, in the definition of the auto-covariance density to handle the singularity in its behaviour at $u=0$ (Bartlett, 1963), and takes the value $P_N/2\pi$ because the $\operatorname{var}[dN(t)] = P_N\, dt$.

An interpretation of the point-process spectra defined by expressions (2.12) and (2.13) may be obtained by considering the empirical Fourier transforms of the point-process data.

The empirical Fourier transform of a sample of duration T from process N with set of spike times $\{\tau_j\}$ is defined as

$$d_N^T(\lambda) = \int_0^T e^{-i\lambda t}\, dN(t) = \sum_{0<\tau_j\le T} \exp\{-i\lambda\tau_j\} \tag{2.14}$$

with a similar expression for the sample process M. The cross-spectrum, $f_{NM}(\lambda)$, between processes N and M is then given by

$$f_{NM}(\lambda) = \lim_{T\to\infty} \frac{1}{2\pi T} E\{d_N^T(\lambda)\, \overline{d_M^T(\lambda)}\} \qquad \lambda \neq 0 \tag{2.15}$$

where the overbar "$\overline{}$" indicates complex conjugate. The auto-spectrum, $f_{NN}(\lambda)$, is obtained by replacing M by N. For T large and $\lambda \neq 0$ the empirical Fourier transform has zero mean (Brillinger, 1983), consequently, from expression (2.15) the cross-spectrum may be seen to have the same form as a covariance parameter, and the auto-spectrum as a variance parameter. Expression (2.15) also leads to a procedure for estimating point-process spectra, as will be seen later.

III. THE COHERENCE AS A MEASURE OF ASSOCIATION

One way to approach measures of association that leads directly to Fourier-based definitions is to consider the problem of predicting some function of one point process from a function of a second point process. For example, consider the problem of predicting the general linear combination

$$\int a(t)\,\mathrm{d}N(t)=\sum_j a(\tau_j) \tag{3.1}$$

of the N-process with spike times $\{\tau_j\}$ by a linear combination,

$$\mu+\int b(s)\,\mathrm{d}M(s)=\mu+\sum_k b(\sigma_k) \tag{3.2}$$

of the M-process with spike times $\{\sigma_k\}$; $a(t)$ and $b(t)$ may be thought of as weighting functions.

It can be shown, by elementary arguments, that the mean-squared error of prediction,

$$E\,|\sum_j a(\tau_j)-\mu-\sum_k b(\sigma_k)|^2 \tag{3.3}$$

is minimized by the choice

$$B(\lambda)=A(\lambda)\frac{f_{NM}(\lambda)}{f_{NN}(\lambda)} \tag{3.4}$$

and that the minimum value achieved is

$$\int |A(\lambda)|^2[1-|R_{NM}(\lambda)|^2]f_{NN}(\lambda)\,\mathrm{d}\lambda \tag{3.5}$$

where $A(\lambda)$ and $B(\lambda)$ denote the Fourier transforms of $a(t)$ and $b(t)$, respectively, and

$$|R_{NM}(\lambda)|^2=\frac{|f_{NM}(\lambda)|^2}{f_{NN}(\lambda)f_{MM}(\lambda)}. \tag{3.6}$$

$|R_{NM}(\lambda)|^2$ is called the coherence of processes N and M at frequency λ. The coherence is symmetric in N and M. It may also be shown to be bounded by 0 and 1, with zero corresponding to the case where knowledge of the M-process is of no use in linearly predicting the N-process. $|R_{NM}(\lambda)|^2=1$ gives a mean-squared error of prediction equal to zero, and corresponds to perfect linear prediction. Incidentally, the parameter

$$S(\lambda)=\frac{f_{NM}(\lambda)}{f_{MM}(\lambda)} \tag{3.7}$$

of expression (3.4) is referred to as the transfer function, at frequency λ, for the prediction.

From expression (2.15) above and the definition of correlation, denoted by "corr", one can see that

$$|R_{NM}(\lambda)|^2=\lim_{T\to\infty}|\mathrm{corr}\{\mathrm{d}_N^T(\lambda),\mathrm{d}_M^T(\lambda)\}|^2. \tag{3.8}$$

Expression (3.8) provides an alternative interpretation of the coherence as the magnitude-squared of the correlation between the empirical Fourier transforms of the processes N and M.

In contrast to expression (3.8), the cross-correlation based approach to measures of association follows directly from a consideration of the correlation between events in one spike-train displaced in time with respect to those in a second train. If $[M(t), N(t)]$ represents a stationary bivariate point process, we can write

$$\mathrm{Corr}\{\mathrm{d}N(t+u),\mathrm{d}M(t)\}$$

to represent the correlation between the two processes, and it then follows from the earlier definitions of Section II that

$$\begin{aligned}\mathrm{Corr}\{\mathrm{d}N(t+u),\mathrm{d}M(t)\}&=(P_{NM}(u)\,\mathrm{d}u\,\mathrm{d}t-P_NP_M\,\mathrm{d}u\,\mathrm{d}t)/(P_NP_M\,\mathrm{d}u\,\mathrm{d}t)^{1/2}\\&=\sqrt{\mathrm{d}u\,\mathrm{d}t}\,q_{NM}(u)/\sqrt{P_NP_M}.\end{aligned} \tag{3.9}$$

Expression (3.9) may be seen to be the basis of the use of the cross-covariance as a measure

of association between spike trains. An indication of the non-normed character of this measure of association is provided by the occurrence of the term $\sqrt{du\, dt}$ in (3.9).

As suggested by the development above, an alternative to the cross-covariance based approach to measures of association is to consider, following (3.8), the behaviour of the correlation between the empirical Fourier transforms of the processes.

In order to be able to make inferences concerning population parameters it is necessary to estimate them using the data, and to have approximations to the sampling fluctuations of these estimates. As an estimate for the cross-spectrum, $f_{NM}(\lambda)$, one can consider, for example,

$$\hat{f}_{NM}(\lambda) = \frac{1}{2\pi LT} \sum_{l=1}^{L} d_N^T(\lambda, l)\, \overline{d_M^T(\lambda, l)} \tag{3.10}$$

where the original time period of observation, of duration LT, has been broken into L disjoint sections each of duration T (Brillinger, 1975b). $d_N^T(\lambda, l)$ denotes the empirical Fourier transform of the events of process N for the l^{th} section. The coherence, $|R_{NM}(\lambda)|^2$, may be estimated by

$$|\hat{R}_{NM}(\lambda)|^2 = \frac{|\hat{f}_{NM}(\lambda)|^2}{\hat{f}_{NN}(\lambda)\hat{f}_{MM}(\lambda)} \tag{3.11}$$

and its statistical significance examined by referring its value to the point $1-(1-\alpha)^{1/(L-1)}$ at each frequency λ, where L is the number of disjoint sections averaged according to the procedure set out above, and α is the desired level of confidence. Values of $|R_{NM}(\lambda)|^2$ less than the level defined by $1-(1-\alpha)^{1/(L-1)}$ can be taken as providing evidence for a lack of a linear association between the processes M and N at that frequency (Brillinger, 1975b).

The quantity $R_{NM}(\lambda) = f_{NM}(\lambda)/(f_{MM}(\lambda) f_{NN}(\lambda))^{1/2}$, whose modulus squared is the coherence, is referred to as the coherency (Wiener, 1930). The phase-spectrum, defined as the argument of the coherency, is given by

$$\phi_{NM}(\lambda) = \arg R_{NM}(\lambda) = \arg f_{NM}(\lambda) = \arg S(\lambda) \tag{3.12}$$

supposing $f_{NN}(\lambda)$ and $f_{MM}(\lambda)$ to be non-zero. As will be shown next, the phase-spectrum may be used to assess the timing relations between processes N and M.

Suppose, for example, that $[\sigma_k, \tau_j]$ represent the spike times for the bivariate process $\{M(t), N(t)\}$. The cross-spectrum between N and M, as seen above, is given by

$$f_{NM}(\lambda) = \lim_{T\to\infty} \frac{1}{2\pi T} E\left(\sum_j e^{-i\lambda\tau_j}\right)\left(\sum_k e^{i\lambda\sigma_k}\right). \tag{3.13}$$

If process N is a lagged version of process M, with lag τ, i.e. $\tau_j = \sigma_j + \tau$, then

$$\begin{aligned} f_{NM}(\lambda) &= \lim_{T\to\infty} \frac{1}{2\pi T} E\left(\sum_j e^{-i\lambda(\sigma_j+\tau)}\right)\left(\sum_k e^{i\lambda\sigma_k}\right) \\ &= e^{-i\lambda\tau} f_{MM}(\lambda) \end{aligned} \tag{3.14}$$

so that

$$\phi_{NM}(\lambda) = -\lambda\tau. \tag{3.15}$$

Therefore, in the case of a pure delay, $\phi(\lambda)$ is proportional to λ, with τ, the delay, equal to the constant of proportionality. If $\tau = 0$, the two processes N and M would be synchronous, and one could expect the sample phase-spectrum to be close to zero. The application of expression (3.15) is valid in the large number of cases where the relation between two spike-trains can be assumed to be dominated by a delay, and where the fitted linear phase curve fits the estimated phase-spectrum quite well. If $\lambda \neq \mu$ and $0 < \lambda, \mu < \pi$, then the $\text{cov}\{\hat{\phi}(\lambda), \hat{\phi}(\mu)\} \doteq 0$ (Brillinger, 1975b), and, therefore, the delay between processes N and M may be well estimated as the slope of the least-squares line relating $\phi(\lambda)$ to λ, taking suitable note of the fact that the phase is only defined up to a multiple of 2π.

The phase-spectrum may be estimated from the estimated cross-spectrum between the two processes. If the spectral estimation procedure set out above is followed, then an approximate 95% confidence interval for the phase at frequency λ may be set as,

$$\Phi^T_{NM}(\lambda) \pm 1.96\left[\frac{1}{L}\left(\frac{1}{|R^T_{NM}(\lambda)|^2} - 1\right)\right]^{1/2} \tag{3.16}$$

where L is again the number of disjoint sections averaged.

IV. EXAMPLES OF COHERENCE AND PHASE

The examples to be presented in this section illustrate several ways in which the coherence provides useful additional information about interactions between spike trains beyond that given by the cross-intensity function. Although the coherence may be considered in some ideal sense as mathematically equivalent to the cross-intensity, that is only true for the population parameters. When one is working with data, however, they display features differently and the sample coherence may well represent important features of the data more clearly than the sample cross-intensity. The usefulness of both time- and frequency-domain representations of a data-set has already been illustrated for the auto-intensity compared with the auto-spectrum by Brillinger *et al.* (1976) and Rosenberg and Rigas (1985).

The following examples are based on experiments in collaboration with M. H. Gladden on cat tenuissimus muscle spindles where the primary (Ia) and secondary (II) endings from the same spindle were isolated in dorsal root filaments following a modification of a procedure introduced by Bessou and Laporte (1963). Single static fusimotor axons (γ_s) were isolated in cut ventral root filaments. Static fusimotor axons were stimulated separately or independently and concurrently with sequences of pulses derived from Geiger counters driven by separate radioactive sources. The length of the parent muscle containing the muscle spindle could be altered by a servo-controlled muscle stretcher. In our experiments random length changes were imposed on the parent muscle. The random length changes had a Gaussian distribution of amplitudes and a constant spectral density over the range 0–100 Hz. The responses of the Ia and II sensory endings were recorded simultaneously during stimulation of one or several fusimotor axons in the presence and absence of a concomitant random length change or in the presence of a length change alone. The preliminary physiological results of these experiments have been presented elsewhere (Halliday *et al.*, 1988).

Figure 1 illustrates the application of both cross-intensity (Fig. 1a, b) and coherence (Fig. 1c, d) to the same data-set to provide a comparison of the effects that each of two static fusimotor axons has alone on the response of the same Ia sensory ending during concurrent and independent stimulation of both fusimotor axons with the parent muscle held at a fixed length. In this example the two cross-intensities (Fig. 1a, b) differ both in shape and in peak value. The ratio of $P_{NM}(u)/P_N P_M$ provides one possible time-domain measure of the strength of association between two point-processes (Brillinger, 1975a). Sears and Stagg (1976) used the maximum value of this ratio, referred to by them as the k-value, to assess the strength of association between two spike trains. For example, the cross-intensity represented in Fig. 1a has a k-value of 2.56, whereas the k-value for the cross-intensity represented in Fig. 1b is 3.26. The coherences confirm this difference in the strength of association, but also allow a further characterization of the differences between the effects of the two fusimotor axons on the same Ia ending. The coherences (Fig. 1c, d) suggest that ${}_2\gamma_s$ has a stronger effect on the Ia ending than ${}_1\gamma_s$ at each frequency over a broad range of frequencies.

The range of frequencies over which the the strength of coupling of the two fusimotor axons to the Ia ending differ can be made more precise by the introduction of a simple statistical test. Brillinger (1975b, chap. 8) demonstrated that for two bivariate processes, under the hypothesis that $|R_{AB}(\lambda)| = |R_{CD}(\lambda)|$, for all values of λ, that $\{\text{Tanh}^{-1}|R_{AB}(\lambda)| - \text{Tanh}^{-1}|R_{CD}(\lambda)|\}$ will be, for T large, approximately normally distributed with zero mean and variance $1/L$, where L is the number of periodograms averaged in the computation of the components of $|R_{AB}(\lambda)|$ and $|R_{CD}(\lambda)|$. When $|R_{AB}(\lambda)|$ and $|R_{CD}(\lambda)|$ are estimated from independent experiments one may plot the standardized difference of the moduli of the transformed coherencies and investigate the hypothesis that $|R_{AB}(\lambda)| = |R_{CD}(\lambda)|$ by referring

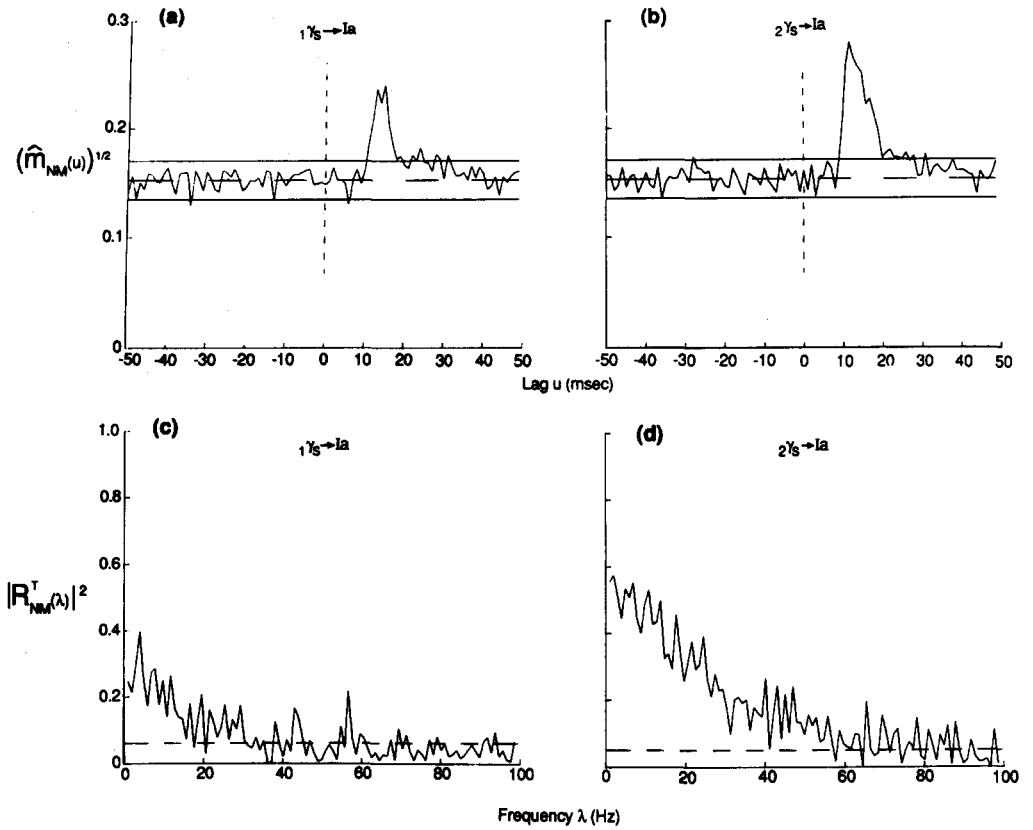

FIG. 1. Comparison of (a, b) the square-root of the estimated cross-intensity functions with (c, d) the estimated coherences of the response of a muscle spindle Ia sensory ending to concurrent and independent stimulation of two static fusimotor axons denoted as $_1\gamma_s$ and $_2\gamma_s$. The fusimotor axons were stimulated for periods of 60 sec, with sequences of pulses having an exponential distribution of intervals. In (a, b) the horizontal dashed line is the asymptotic value of the square-root of the estimated cross-intensity function equal to the square-root of the mean rate of the Ia discharge. The horizontal solid lines represent an approximate 95% confidence interval for the value of the cross-intensity function for any specific value of the lag u under the assumption that the two processes are independent (Brillinger *et al.*, 1976). In (c, d) the horizontal dashed line represents the upper level of the approximate 95% confidence interval for the coherence for any specific value of the frequency λ under the hypothesis that the two processes are independent (Brillinger, 1975b, chap. 8).

the value of this difference for any given value of λ to the value of a standardized normal variate at, say, the 5% level of significance. Figure 2 gives an example of the difference plot corresponding to the coherences illustrated in Fig. 1c, d. Under the hypothesis of equal coherences an approximate 95% confidence interval is represented by the horizontal solid lines in Fig. 2. Points that lie outside this interval indicate frequencies where the difference between the strength of association of the pair of processes may plausibly be inferred to be non-zero. The difference plot (Fig. 2) suggests that the two coherences shown in Fig. 1c, d exhibit a small but significant difference over the range from 0 to about 20 Hz. Over this range of frequencies $_2\gamma_s$ is more strongly coupled to the Ia ending than $_1\gamma_s$. Above about 20 Hz the difference between the two coherences is not significant.

The covariance structure of the estimate for the cross-intensity does not allow this type of test to be constructed easily (Torres-Melo, 1974). Therefore, in addition to providing a normative measure of the strength of association between two processes (a property not possessed by the k-measure of the strength of association between two spike trains) the modulus of the coherency may be transformed and used to express the difference between the strengths of association between pairs of processes.

The second example compares cross-intensities with coherences in describing the effects of independent stimulation of two fusimotor axons on the responses of the Ia and II endings from the same muscle spindle. Fusimotor stimulation occurred in the presence of a

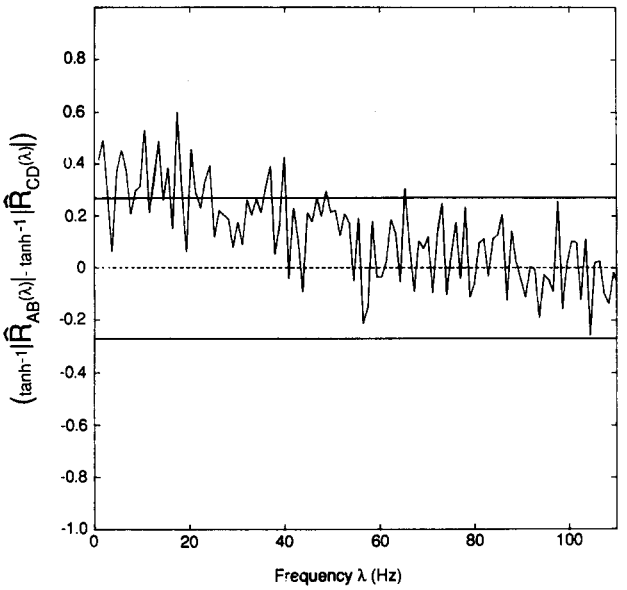

FIG. 2. Graph of the difference of the $\tanh^{-1}$ of the moduli of the coherencies corresponding to the estimated coherences shown in Fig. 1c, d along with the approximate 95% confidence interval—solid horizontal lines—for the hypothesis that the two moduli are equal at any given frequency λ. Points lying outside this interval indicate frequencies where the difference between the strength of association of the pair of processes may plausibly be non-zero.

randomly varying length change applied to the parent muscle containing the spindle. In this situation one would expect the structure of the cross-intensities to be different. The only apparent difference, however, is that in the presence of three inputs applied simultaneously to the muscle spindle the Ia ending discharges at a higher rate in response to the ${}_1\gamma_s$ ending (Fig. 3a) than the II ending discharges in response to the ${}_2\gamma_s$ ending (Fig. 3b). The two coherence plots (Fig. 3c, d), on the other hand, demonstrate that the ${}_1\gamma_s$ is not coupled to the Ia response, which is also obvious in Fig. 3a, but that ${}_2\gamma_s$ exhibits a small but significant coupling to the II ending at low frequencies, which is not apparent from the estimated cross-intensity for the same case (Fig. 3b).

The phase curve for the relationship between fusimotor input and the response of the II ending is taken as the argument of the estimated coherency corresponding to the coherence shown in Fig. 3d. The estimated phase is approximately linear over the range where the coherence for this relation is significant (Fig. 4). Above about 15 Hz the estimated phase curve oscillates erratically about the zero phase line, indicating the absence of coupling between the two processes (Jenkins and Watt, 1968). The slope of the linear phase curve gives an estimated delay of 29.8 msec, uncorrected for conduction delays, with a 95% confidence interval about the estimate equal to 29.8 ± 2.18 msec.

Figure 4 is a dramatic example of the use of a frequency-domain measure to estimate a time-domain parameter in a situation where the same parameter could not be estimated from the direct time-domain measurement. Even in cases more favourable to the use of the cross-intensity function for estimating the time delay, Fig. 1a, b, for example, its determination depends on the estimation of the time of occurrence of a single point, the peak of the cross-intensity curve, whereas the delay estimated from the phase curve takes into account more of the information in the data. In addition, one can use regression theory to estimate the standard error of the estimated delay. In situations where the coherence is not constant, weighted least-squares would have to be used (see Appendix). Therefore, even when the peak of the cross-intensity may be reasonably well-defined it is better to estimate delays from the phase curve, where one can also determine the standard error of the estimate. (For an estimate to be useful one needs an estimate of its uncertainty.)

The next two examples illustrate, in a qualitative manner, how the coherence may be used to assess changes in the relation between two processes brought about by the addition of

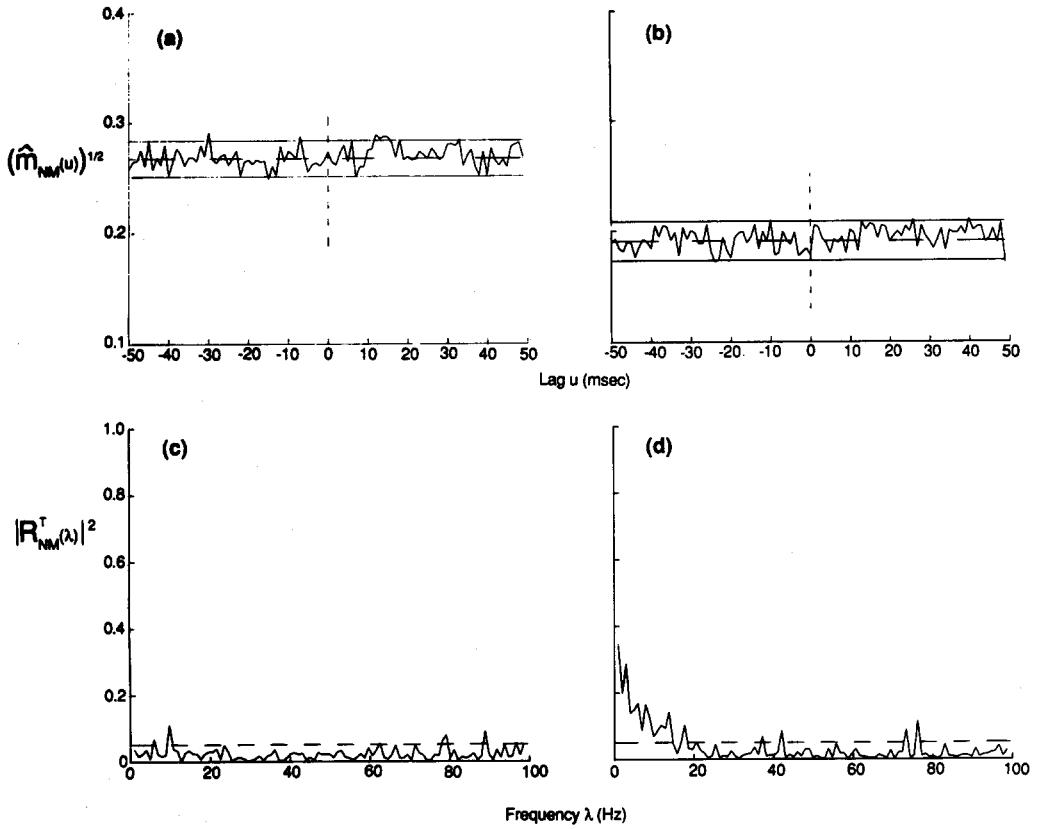

FIG. 3. Comparison of (a, b) the square-root of the estimated cross-intensity functions with (c, d) the estimated coherences of the response of the Ia and II sensory endings from the same muscle spindle to independent stimulation of two static fusimotor axons ($_1\gamma_s$ and $_2\gamma_s$) during the presence of a randomly varying length change imposed on the parent muscle. The estimates in (a) and (c) are computed for the Ia response to $_1\gamma_s$, and those in (b) and (d) for the II response to $_2\gamma_s$ stimulation. Approximate 95% confidence intervals for the value of the cross-intensity function for any specific value of the lag u—horizontal solid lines—are set as for Fig. 1.

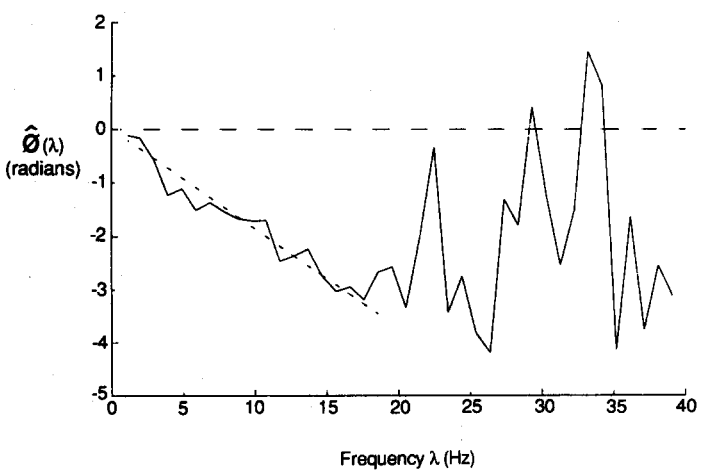

FIG. 4. Estimated phase, $\hat{\Phi}(\lambda)$, for the response of a muscle spindle II ending to stimulation of a static fusimotor axon. The coherence for the same relation is illustrated in Fig. 3d. The dashed line represents the linear regression line fitted to the phase curve over the range of frequencies where the coherence shown in Fig. 3d is significant. The slope of the linear phase curve gives an estimated delay of 29.9 msec with 95% confidence limits of 29.9 ± 2.18 msec.

other processes. Figure 5 illustrates how the coupling between one static fusimotor axon and the Ia and II endings from the same muscle spindle is influenced by the presence of a second fusimotor input and a continuously varying length change imposed on the parent muscle. Figure 5a compared with Fig. 5b shows that ${}_1\gamma_s$ is coupled to both the Ia and II endings with approximately the same maximum strength, but that the coupling occurs over a slightly broader frequency range in the case of the ${}_1\gamma_s$ onto the Ia ending. The activation of a second static fusimotor axon, ${}_2\gamma_s$ (Fig. 5c, d), reduces, significantly, the strength of the coupling of ${}_1\gamma_s$ onto the Ia at all frequencies below about 40 Hz (Fig. 5b compared with Fig. 5d), whereas the presence of ${}_2\gamma_s$ activity has only a very small effect on the ${}_1\gamma_s$ to II coherence at frequencies less than about 5 Hz (Fig. 5a compared with Fig. 5c). The ${}_1\gamma_s$ to II coupling remains unchanged following the addition of the length input to the parent muscle along with the stimulation of ${}_2\gamma_s$ (Fig. 5c compared with Fig. 5e), whereas under the same multiple input conditions ${}_1\gamma_s$ activity becomes completely uncoupled from the Ia response (Fig. 5d compared with Fig. 5f). In this example the addition of a length input causes only a very small increase in the mean rate of discharge of the II ending, but more than doubled the Ia rate, although the ${}_1\gamma_s$ activity became uncoupled from that of the Ia ending (Fig. 5f). This example suggests that within the same muscle spindle the II ending is largely unaffected by the presence of a dynamic length change imposed on the spindle while remaining strongly coupled to the fusimotor input, whereas the Ia ending becomes uncoupled from ${}_1\gamma_s$ and responds to a combination of the dynamic length change and the ${}_2\gamma_s$ input. This interpretation of the results set out in Fig. 5 is consistent with the known differences in the behaviour of Ia and II endings of the muscle spindle examined separately in response to dynamically imposed length changes (e.g. Matthews, 1981), with the additional information that the II ending, in the presence of dynamic length changes still responds primarily to the fusimotor imputs, and that the Ia ending responds to only one of the static fusimotor axons activated simultaneously with the length change, although it responds to both static fusimotor axons alone. These observations highlight the difficulty in making inferences about the behaviour of a complex system like the muscle spindle based on observations from single input single output experiments.

Figure 6 illustrates how the coupling between two output processes, the Ia and II endings from the same spindle, depends on the input conditions imposed on the spindle. In the presence of the independent stimulation of two static fusimotor axons the Ia and II endings are coupled in the range from about 1–18 Hz (Fig. 6a), whereas in the presence of a dynamically changing length signal the Ia and II endings are coupled over the range of approximately 20–60 Hz (Fig. 6b). If all three inputs are present, two distinct regions of coupling between Ia and II occur—a low-frequency, fusimotor-dependent range of frequencies and a second distinctly different length-dependent range of higher frequencies (Fig. 6c).

It is also of interest, in the light of recent work by Edgley and Jankowska (1987), to examine how the phase relation between Ia and II responses to fusimotor input becomes altered by changes in fusimotor input. In this example the delay estimated from the phase between Ia and II responses, computed in the presence of ${}_1\gamma_s$ (Fig. 7c) is 2.45 msec—a phase lead of Ia over II—over the range of frequencies where the coherence shows significant coupling between the Ia and II endings (Fig. 7a). This small difference in phase between the Ia and II responses at the level of input to the spinal cord, where their activity was recorded, occurred in spite of the large difference in their respective conduction velocities. On the other hand, in the presence of ${}_2\gamma_s$ alone (Fig. 7d), there is a significantly larger phase lead of the Ia response over that of the II response over the range of frequencies where the Ia–II coherence is significant (Fig. 7b). This phase lead corresponds to a delay of 16.1 ± 2.9 msec which is substantially greater than one would expect on the basis of conduction velocity differences alone. The significance of this result has been discussed elsewhere (Halliday *et al.*, 1988).

V. THE COHERENCE AS A MEASURE OF PARTIAL ASSOCIATION

The examples presented in Section IV indicate, in a qualitative manner, how the coherence and phase may be used to demonstrate the alterations that occur in the strength of

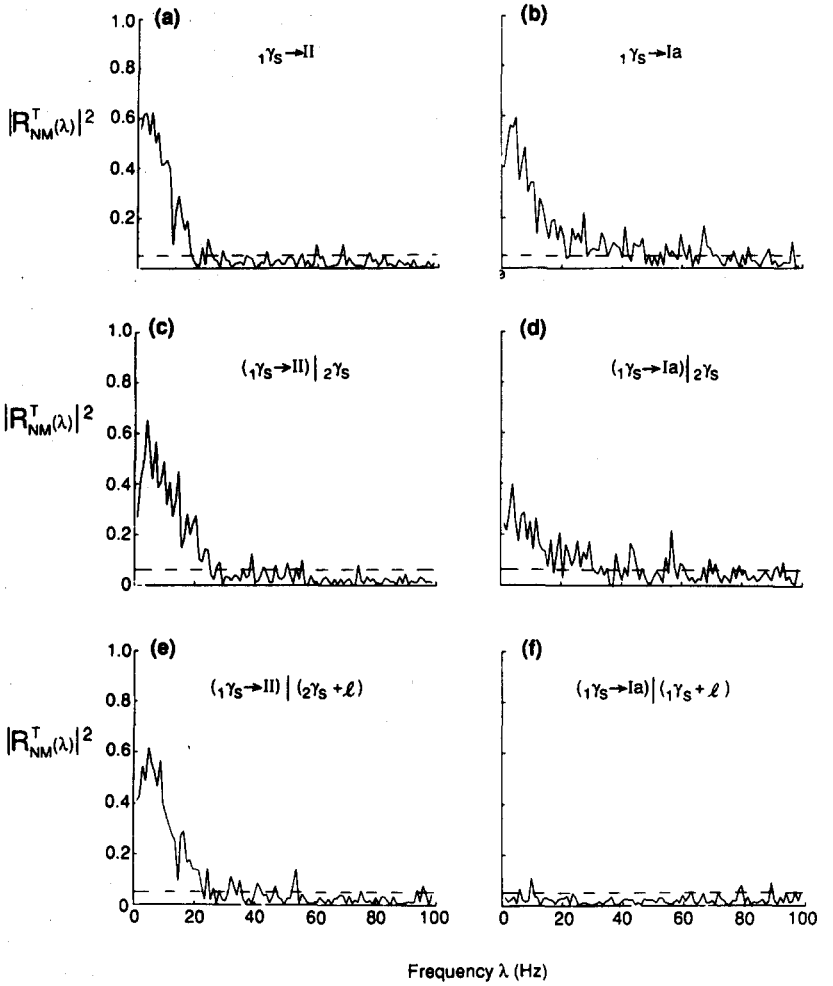

FIG. 5. Estimated coherences between the responses of Ia and II sensory endings from the same muscle spindle (a, b) to stimulation of a single static fusimotor axon, (c, d) to stimulation of the same static fusimotor axon, and (e, f) in the presence of the stimulation of a second static fusimotor axon during the application of a random length change to the parent muscle. The fusimotor axons were stimulated independently for 60 sec at the same mean rate with sequences of pulses having an exponential distribution of intervals. The horizontal dashed lines in each panel indicate the upper level for the approximate 95% confidence interval for the coherence for any specific value of the frequency λ under the hypothesis that the two processes are independent.

association and timing relations between two processes brought about by the presence of other factors. The method used in Section IV to derive the coherence may be extended to allow the consideration of a broader class of questions than those discussed in that section, and which only examined changes in coherence and phase between two processes brought about by the direct activation of experimentally accessible inputs to the muscle spindle.

It is not always possible, however, to add, remove or hold constant a process that is suspected of influencing the relation between other processes. It may, however, be possible to record its activity. Suppose, for example, that three point processes, L, M, N are found to be pairwise associated; can it be inferred that the observed relation between some two, say M and N, is a consequence of a common input L, or that it is simply the result of a direct connection between M and N? The partial coherence provides a means of answering this question.

It was shown in Section III that the coherence, $|R_{NM}(\lambda)|^2$, provides a measure of how well a linear combination of the N-process (3.1) could be predicted from a linear combination of the M-process (3.2).

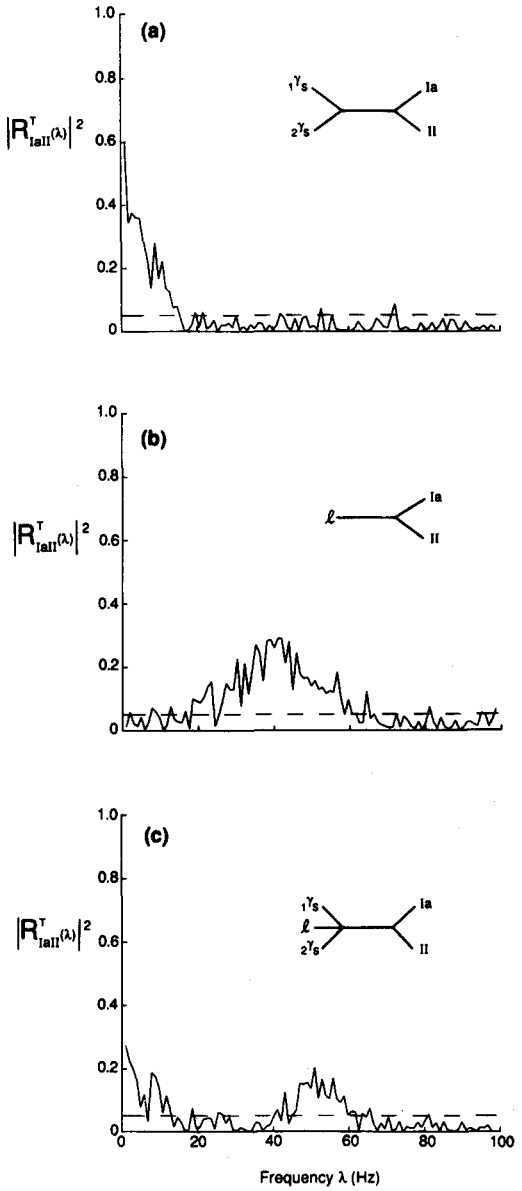

FIG. 6. The estimated coherence between the responses of a Ia and II sensory ending from the same muscle spindle (a) during independent stimulation of two static fusimotor axons, (b) in the presene of an imposed random length change, and (c) in the presence of both fusimotor stimulation and the imposed length change. The horizontal dashed line in each panel indicates the upper level for an approximate 95% confidence interval for the coherence for any specific value of the frequency λ under the hypothesis that the two processes are independent.

The partial coherence, $|R_{NM/L}(\lambda)|^2$, provides a measure of how much this prediction is improved by M if a linear combination of the L-process,

$$\int c(r)\,\mathrm{d}L(r) \tag{5.1}$$

is also included in predicting the linear combination of the N-process.

Following the method of Section III, one now considers the problem of predicting

$$\int a(t)\,\mathrm{d}N(t) \tag{5.2}$$

by the linear combination

$$\mu+\int b(s)\,\mathrm{d}M(s)+\int c(r)\,\mathrm{d}L(r) \tag{5.3}$$

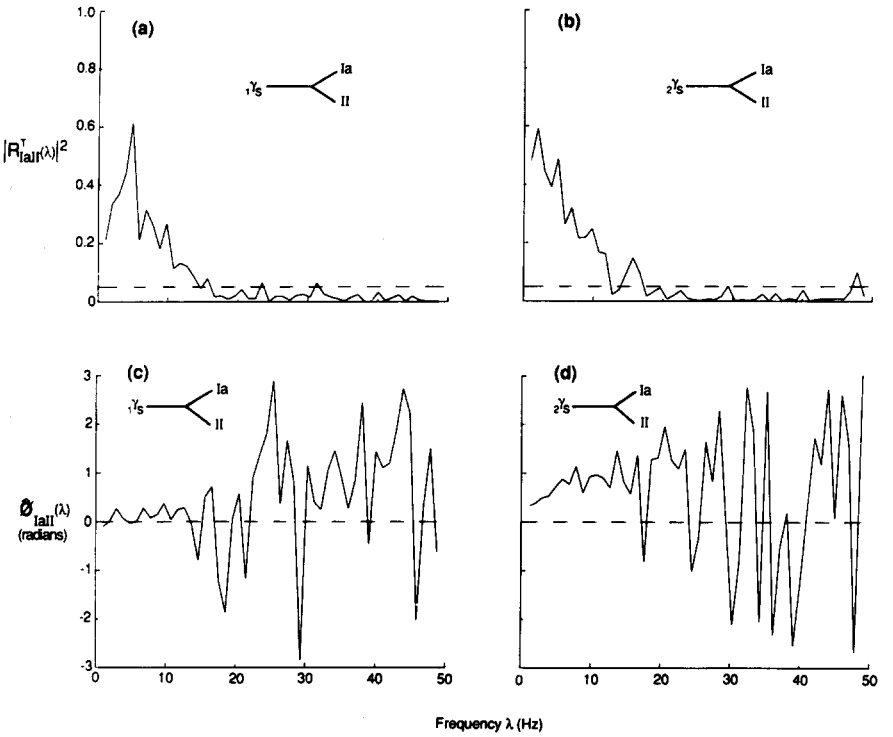

FIG. 7. The estimated coherence (a, b) and phase (c, d) between the responses of a Ia and II ending from the same muscle spindle during stimulation of two different static fusimotor axons as indicated. The fusimotor axons were stimulated for 60 sec with sequences of pulses having an exponential distribution of intervals. The horizontal dashed lines in (a, b) indicate the upper level for the approximate 95% confidence interval for the coherence for any specific value of the frequency λ under the hypothesis that the two processes are independent.

where $a(t)$, $b(t)$ and $c(t)$ are weighting functions as in Section III.

In this example the minimum mean-squared error may be written as

$$\int |A(\lambda)|^2[1-|R_{N\cdot ML}(\lambda)|^2]f_{NN}(\lambda)\,d\lambda \tag{5.4}$$

where

$$|R_{N\cdot ML}(\lambda)|^2=|R_{NL}(\lambda)|^2+|R_{NM/L}(\lambda)|^2[1-|R_{NL}(\lambda)|^2] \tag{5.5}$$

is the multiple coherence at frequency λ of the process N on the processes M and L, which takes into account the fact that two processes are now being used to predict a third (Brillinger, 1975b; Jenkins and Watt, 1968).

$|R_{NM/L}(\lambda)|^2$ in (5.5) is called the partial coherence of processes N and M in the presence of process L. It may be explained as the relative improvement of predicting N from M at frequency λ having already taken into account process L, and can be written in terms of ordinary coherences, suppressing the dependencies on λ for simplicity in writing, as

$$R_{NM/L}=\frac{R_{NM}-R_{NL}R_{LM}}{[(1-|R_{NL}|^2)(1-|R_{LM}|^2)]^{1/2}}. \tag{5.6}$$

The partial coherence also has limits between 0 and 1, with 0 now corresponding to the situation where the relation between N and M is entirely accounted for by taking into account their individual dependencies on process L.

The Fourier transforms of the functions $a(\cdot)$, $b(\cdot)$, and $c(\cdot)$ above satisfy the normal equations

$$B(\lambda)f_{MM}(\lambda)+C(\lambda)f_{LM}(\lambda)=A(\lambda)f_{NM}(\lambda) \tag{5.7a}$$

$$B(\lambda)f_{ML}(\lambda)+C(\lambda)f_{LL}(\lambda)=A(\lambda)f_{NL}(\lambda). \tag{5.7b}$$

Suppressing the dependencies on λ, one has

$$B = A\frac{f_{NM}f_{LL} - f_{NL}f_{LM}}{f_{MM}f_{LL} - f_{LM}f_{ML}}. \tag{5.8}$$

The question of whether the L-process provides any improvement in predicting the N-process from the M-process may now be formulated as the question of whether $B \equiv 0$. B may be shown to be a multiple of the partial coherency, $R_{NM/L}(\lambda)$, as $B(\lambda)$ of (3.4) is a multiple of the ordinary coherency $R_{NM}(\lambda)$. For variants of these "partial" quantities in the case of ordinary random variables see Kendall and Stuart (1961, chap. 27).

One may define the partial phase as

$$\Phi_{NM/L}(\lambda) = \arg\{R_{NM/L}(\lambda)\} = \arg\{f_{NM/L}(\lambda)\}. \tag{5.9}$$

Expression (5.9) may be written in terms of the basic spectra of the component processes, since

$$f_{NM/L}(\lambda) = f_{NM}(\lambda) - \frac{f_{NL}(\lambda)f_{LM}(\lambda)}{f_{LL}(\lambda)} \tag{5.10}$$

where $f_{NM/L}(\lambda)$ is defined as the partial cross-spectrum between processes N and M taking into account process L (Tick, 1963). Partial auto-spectra are defined by equating N and M in expression (5.10).

If one considers the problem of predicting the contribution that the L-process makes to each of the processes M and N on the basis of a linear time-invariant point-process model (Brillinger, 1975a), then the partial coherence may be written, suppressing the dependencies on λ, as

$$|R_{NM/L}|^2 = \lim_{T\to\infty} \left|\operatorname{corr}\left\{d_N^T - \frac{f_{NL}}{f_{LL}}d_L^T,\ d_M^T - \frac{f_{ML}}{f_{LL}}d_L^T\right\}\right|^2 \tag{5.11}$$

where f_{NL}/f_{LL}, f_{ML}/f_{LL} may be thought of as regression coefficients giving the best linear predictors of d_N^T and d_M^T in terms of d_L^T for large T. The development of expression (5.11) leads to (5.6). The partial coherence may now be seen to be the correlation between the Fourier transforms of the N and M processes after removing the linear time-invariant contribution that process L makes to each of these processes.

VI. EXAMPLES OF PARTIAL COHERENCE, PARTIAL SPECTRA AND PARTIAL PHASE (ORDER-1)

The following examples demonstrate several practical applications of partial coherence, partial spectra and partial phase, first to computer generated data and then to real data taken from experiments on mammalian muscle spindles. In the first example a simple neuronal network is simulated on an analog computer in which two model neurones, simulated by an "integrate to threshold and fire model" (e.g. Holden, 1976), have a common excitatory input, $N_1(t)$, in addition to another independent input. In the absence of the common input, the spike trains of the two neurones are independent. The common input to the model neurones is derived from the response of a Geiger counter driven by a radioactive source, and may therefore be considered as a realization of a Poisson process. In the presence of the shared input the discharge of each neurone, denoted by $N_2(t)$ and $N_3(t)$, has two components—one dependent on the input process and the other independent of this process. These two components are themselves independent. The structure of the simulation corresponds to the assumptions (5.1–5.3) for the model of partial coherence. The sequence of input pulses to the model neurones and the corresponding output pulse sequences from each model neurone were recorded on FM tape and subsequently digitized to give computer files containing the ordered times of occurrence of events for each process. The ordinary pairwise coherences (Fig. 8a, b, c), computed according to expression (3.6), show that the three processes are pairwise coupled. The partial coherence between the outputs of the pair of model neurones

taking into account the input process, (Fig. 8d), demonstrates that the coupling between the discharge of the two neurones is due entirely to the presence of the common input. In the case of three processes, therefore, the partial coherence may be used to identify the presence of a common input (of one sort).

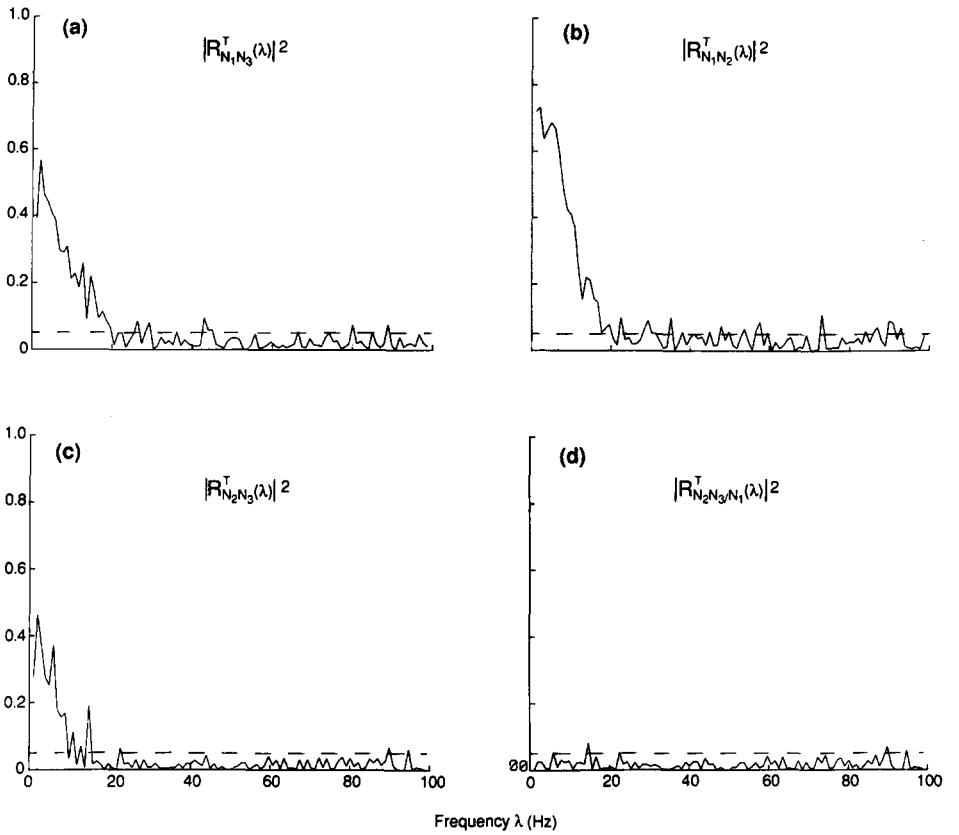

FIG. 8. An example of the application of partial coherence to spike trains derived from model neurones (see text for details of model structure) in response to a common random spike train. N_1 represents the input process common to both model neurones, whose output processes are denoted as N_2 and N_3. (a, b, c) Estimated pairwise coherences, (d) estimated partial coherence between N_2 and N_3 taking into account the contribution from process N_1. The horizontal dashed line indicates the upper level of the approximate 95% confidence interval for the partial coherence for any specific value of the frequency λ under the assumption that the two processes are independent.

A simple example of partial coherence, applied to real data, is taken from the case where the responses of a primary (Ia) and secondary (II) ending from the same muscle spindle are recorded during stimulation of a static fusimotor axon innervating the muscle spindle (Gladden *et al.*, unpublished observations). In the absence of fusimotor stimulation the discharge of the Ia and II endings were uncorrelated, whereas in the presence of fusimotor stimulation, as would be expected, they are strongly correlated (Fig. 9c) over the range of frequencies determined by the coupling of the fusimotor input to the Ia and II endings (Fig. 9a, b). Figure 9d, the partial coherence between the responses of the Ia and II endings taking into account the presence of the fusimotor input, shows that the coupling between these responses is due entirely to the presence of fusimotor stimulation.

In some situations it is also useful to examine partial spectra as well as the partial coherences. Christakos *et al.* (1984), for example, presented some work in which they attempted to identify the contribution that different motor units make to the discharge of a single afferent from a muscle spindle. They attributed peaks at particular frequencies in the auto-spectrum of the Ia discharge to the effects of stimulating single motor units at these frequencies.

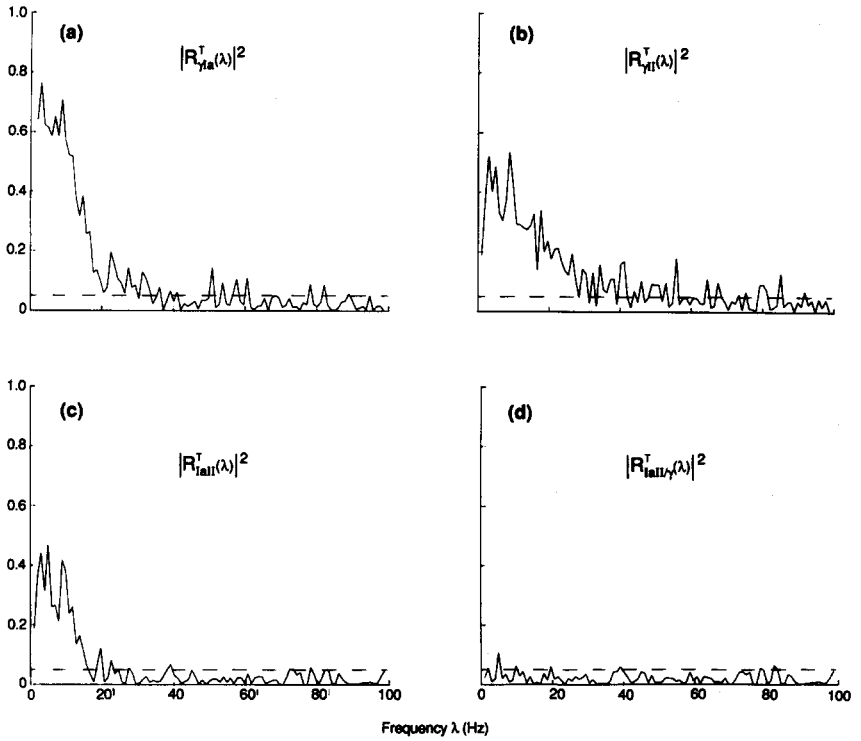

FIG. 9. (a)–(c) The estimated pairwise coherences between a fusimotor input and the responses of Ia and II sensory endings from the same muscle spindle. (d) The estimated partial coherence between the responses of the Ia and II endings taking into account the presence of the static fusimotor input. The static fusimotor axon was stimulated for 60 sec with a sequence of pulses having an exponential distribution of intervals. The horizontal dashed line in each panel represents the upper level of an approximate 95% confidence interval for the coherences for any specific value of the frequency λ under the assumption that the two processes are independent.

The partial spectra allow studies of this kind to be extended to experiments where the activity of several motor units is recorded simultaneously with that of the discharge of a single muscle spindle afferent. It then becomes of interest to determine if any or all of these motor units affect the Ia discharge. Figure 10a is the auto-spectrum of the discharge of a single spontaneously active Ia afferent from a gastrocnemius muscle spindle recorded in continuity with the spinal cord and simultaneously with two motor units from the same muscle (Amjad *et al.*, unpublished observations). The two motor units were firing almost synchronously at about 12 Hz. The peak in the Ia auto-spectrum (Fig. 10a) at this frequency suggests that one or both of these motor units influences the Ia discharge. The partial auto-spectrum taking into account the activity from one of the motor units (α_1) (Fig. 10b) remains largely unchanged, and indicates that this motor unit does not significantly contribute to the Ia discharge. The partial auto-spectrum of the Ia discharge taking into account the activity of the other motor unit (α_2) (Fig. 10c), however, shows a substantial reduction in the peak at 12 Hz suggesting that this motor unit contributes significantly to the Ia discharge. The residual peak at 12 Hz in this partial auto-spectrum further suggests the possibility of the presence of other motor units whose activity influences the Ia discharge.

This example is particularly interesting because the two motor units were themselves coupled, and the cross-intensity between either of them and the Ia discharge would indicate that both affect the Ia discharge. The auto-spectra of the two motor units, however, were different, and consequently the partial auto-spectra could be used to demonstrate that only one of the motor units was effective in modulating the Ia firing rate. This example illustrates a situation in which the use of cross-intensity alone may have been misleading.

The partial coherence only gives information on how the strength of coupling between two processes may be influenced by the action of a third process, and the magnitude of the partial

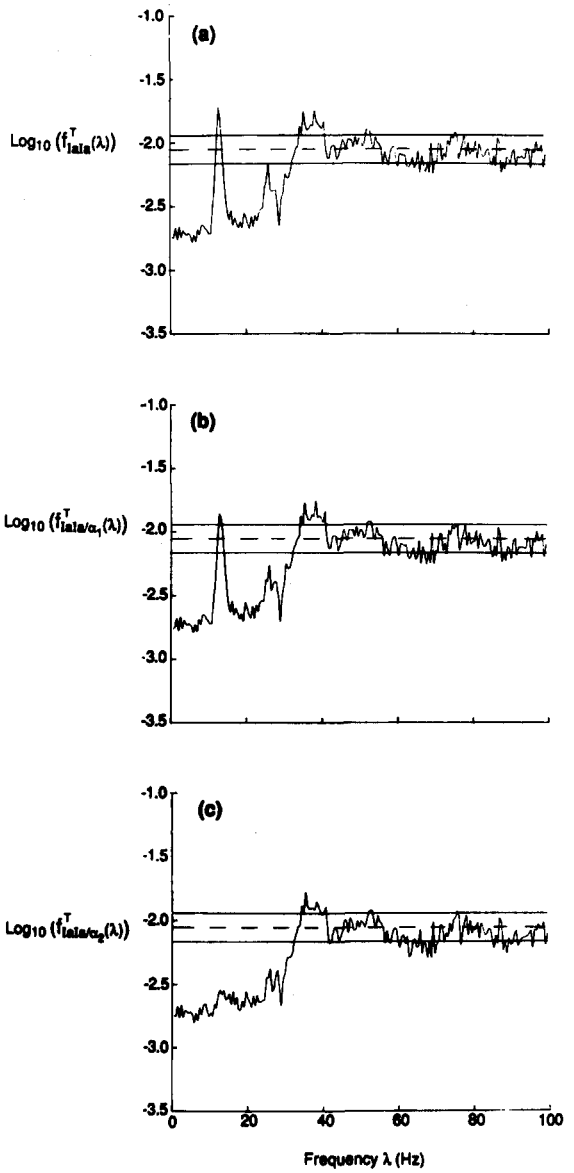

FIG. 10. (a) The estimated auto-spectrum, $f_{IaIa}(\lambda)$ of a spontaneously discharging Ia afferent from a muscle spindle in the gastrocnemius muscle recorded in continuity with the spinal cord along with the recorded activity from two single motor units from the same muscle. (b) Estimated first-order partial auto-spectrum of the Ia discharge taking into account the presence of the discharge of one of the motor units, $(\alpha_1), f_{IaIa/\alpha}(\lambda)$. (c) Estimated first-order partial auto-spectrum of the Ia discharge taking into account the presence of the discharge of the other motor unit, $(\alpha_2), f_{IaIa/\alpha}(\lambda)$. Solid horizontal lines in (a)–(c) are approximate 95% confidence intervals for the auto-spectra. Estimates are plotted on log scale.

spectra allows the identification of contributions that one process may make to another. Neither of these measures provide information on how the timing relations between two processes may be altered by the activity of a third process. Controlled changes in the relative timing between two spike trains that converge onto the same neurone, however, can have a strong effect on regulating the output of this common neurone. The partial phase is a parameter which provides a measure of the extent to which the timing between two spike trains is influenced by a third.

An understanding of how partial phase works may be obtained by considering four spike-trains constructed in the following manner. Let $N_1(t)$ and $N_2(t)$ be two independent Poisson processes with the same mean rates. Process $N_3(t)$ is formed as the superposition of $N_1(t)$ and $N_2(t)$, that is, $N_3(t) = N_1(t) + N_2(t)$. Process $N_4(t)$ is the superposition of delayed versions of

processes $N_1(t)$ and $N_2(t)$, so that $N_4(t)=N_1(t+d_1)+N_2(t+d_2)$, where d_1 and d_2 represent the delay times. Consider processes $N_1(t)$ and $N_2(t)$ as inputs to, and processes $N_3(t)$ and $N_4(t)$ as outputs from a linear time-invariant point process system.

By elementary manipulations one has

$$f_{43}(\lambda)=e^{-i\lambda d_1}f_{11}(\lambda)+e^{-i\lambda d_2}f_{22}(\lambda) \tag{6.1}$$

$$f_{41}(\lambda)=e^{-i\lambda d_1}f_{11}(\lambda) \tag{6.2}$$

$$f_{42}(\lambda)=e^{-i\lambda d_2}f_{22}(\lambda) \tag{6.3}$$

$$f_{31}(\lambda)=f_{11}(\lambda)=f_{13}(\lambda) \tag{6.4}$$

and

$$f_{32}(\lambda)=f_{22}(\lambda)=f_{23}(\lambda). \tag{6.5}$$

From expression (5.10) we can write the partial cross-spectrum, $f_{43/1}(\lambda)$, i.e. the cross-spectrum between processes $N_4(t)$ and $N_3(t)$ after having accounted for process $N_1(t)$, as

$$f_{43/1}(\lambda)=f_{43}(\lambda)-\frac{f_{41}(\lambda)f_{13}(\lambda)}{f_{11}(\lambda)}. \tag{6.6}$$

Substituting expressions (6.1), (6.2) and (6.4) into (6.6) gives

$$f_{43/1}(\lambda)=e^{-i\lambda d_2}f_{22}(\lambda) \tag{6.7}$$

from which it follows that the partial phase, $\Phi_{43/1}(\lambda)$, is

$$\Phi_{43/1}(\lambda)=\arg\{f_{43/1}(\lambda)\}=-\lambda d_2. \tag{6.8}$$

Similarly, the partial phase, $\Phi_{43/2}(\lambda)$ is

$$\Phi_{43/2}(\lambda)=\arg\{f_{43/2}(\lambda)\}=-\lambda d_1. \tag{6.9}$$

The partial phases given by (6.8) and (6.9) are the phases that one would expect between processes $N_3(t)$ and $N_4(t)$ if only one of the input processes were present—refer to expression (6.1).

The phase, $\Phi_{43}(\lambda)$ is

$$\Phi_{43}(\lambda)=\arg\{f_{43}(\lambda)\}=\tan^{-1}\left\{\frac{\operatorname{Im}f_{43}(\lambda)}{\operatorname{Re}f_{43}(\lambda)}\right\}. \tag{6.10}$$

Substitution of the real and imaginary parts of (6.1) into (6.10) gives, after some simplification,

$$\Phi_{43}(\lambda)=\tan^{-1}\left[\frac{(f_{11}(\lambda)/f_{22}(\lambda))(\sin\lambda d_1)+\sin\lambda d_2}{(f_{11}(\lambda)/f_{22}(\lambda))(\cos\lambda d_1)+\cos\lambda d_2}\right] \tag{6.11}$$

which further reduces to

$$\Phi_{43}(\lambda)=-\lambda\left(\frac{d_1+d_2}{2}\right). \tag{6.12}$$

In the presence of both inputs, the derived delay between processes $N_4(t)$ and $N_3(t)$ will be the average of the delays introduced into each of the processes $N_1(t)$ and $N_2(t)$. Figure 11 shows, on the same graph, the derived phase and partial phases for data from the model described above with $d_1=2$ msec and $d_2=-2$ msec (dashed lines). The same parameters derived from the estimated auto- and cross-spectra are also plotted on the same graph (solid lines). The good agreement between the derived and estimated values of the three phase-curves provides a clear example of how one might interpret the partial phase. In this example, with both inputs present, the delay between processes $N_3(t)$ and $N_4(t)$ is the average of the two delays, whereas mathematically removing the effect of one input results in a delay between processes

$N_3(t)$ and $N_4(t)$ equal to that which would be expected to occur in the presence of a single input, as can be seen from expression (6.1).

The equivalence between mathematically removing the influence of one input and physically removing that same input can also be illustrated with an example from the muscle spindle data. This example takes advantage of the statistical properties of the estimated partial phase to set up a test for zero phase or synchrony between two processes. The estimated phase at any frequency is asymptotically normal with variance given from (3.16), and the covariance between estimates at different frequencies is asymptotically zero. One can then set approximate 95% confidence intervals for the hypothesis that the phase at each frequency is zero. Figure 12a, c illustrates the coherence and phase relations between the responses of a pair of Ia and II sensory endings from the same muscle spindle during independent stimulation of two static fusimotor axons. Figure 12e, which gives the graphical representation of the test for zero phase, suggests that with the exception of frequencies below about 4 Hz the phase is non-zero over the range where the coherence is significant (Fig. 12a). The slope of the phase curve is 6.28 ± 0.26 msec. If the effect on the phase relation between the Ia and II responses to the stimulation of a second static fusimotor axon, $({}_1\gamma_s)$, occurred independently of the effect of stimulating the first fusimotor axon $({}_2\gamma_s)$, then the partial coherence and partial phase, taking into account the effect of ${}_2\gamma_s$, would be similar to the coherence and phase between the Ia and II responses during stimulation of the ${}_1\gamma_s$ alone. In this example, the partial coherence between the Ia and II responses taking into account the presence of ${}_2\gamma_s$ (Fig. 12b) is close to the coherence between the Ia and II endings in the presence of ${}_1\gamma_s$ alone (Fig. 7a, c). The test for zero-phase (Fig. 12f) shows that the partial phase is not significantly different from zero up to about 4 Hz. The slope of this partial phase-curve over the range 0–4 Hz was found not to be significantly different from the slope of the phase curve in Fig. 7c, where only ${}_1\gamma_s$ alone was active.

In this example, the effect of the mathematical removal of the influence of one input is seen to give results very close to the effects of having only the other input present. The real data satisfies the assumptions for the derivation of the partial coherences and phases, and consequently suggests for this particular example that the phase between the Ia and II responses changes additively with the activation of a second fusimotor axon. The fact that the successive recruitment of fusimotor axons to a muscle spindle results in graded changes in the phase between the Ia and II responses from the spindle, can be an important parameter in regulating the output from neurones which receive inputs from both of these axons.

VII. COHERENCE AS A MEASURE OF PARTIAL ASSOCIATION (ORDER-K)

The measures presented in Section V for describing how the predictability of a linear combination of one process from a linear combination of a second process is improved by taking into account the contribution of a third process, may be extended to a consideration of how this prediction may be further improved by bringing into account any number of processes, say $M_1, \ldots, M_{r-1}$. The coherence between the N-process and the M_r-process taking into account $M_1, \ldots, M_k$, where $k \leq r-1$, is referred to as the partial coherence of order-k, and is denoted as $|R_{NM_r/M_1,\ldots,M_k}(\lambda)|^2$.

To facilitate this presentation we set out some additional notation for vector-valued and matrix-valued processes. $M(t)$ represents an r-vector valued point process with component processes $M_1, \ldots, M_r(t)$. $F_{MM}(\lambda)$ is an $r \times r$ matrix of spectral densities, whose principle diagonal consists of the auto-spectra of the components of $M(t)$, and the off-diagonal elements the cross-spectra between these components. $F_{NM}(\lambda)$ is an r-vector with components, the cross-spectra between the N-process and each of the components of $M(t)$.

Following the procedure of Section V one now considers the question of predicting

$$\int a(t)\, \mathrm{d}N(t) \tag{7.1}$$

by the linear combination

$$\mu + \sum_{j=1}^{r} b_j(t)\, \mathrm{d}M_j(t). \tag{7.2}$$

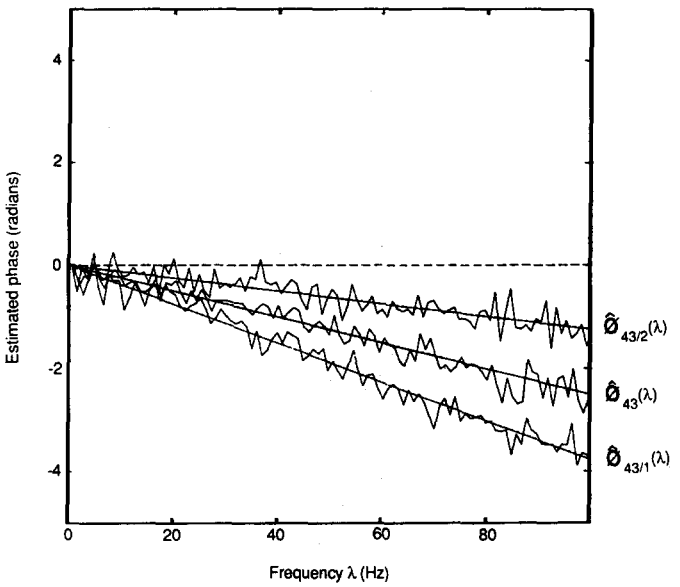

FIG. 11. Derived (dashed lines) and estimated (solid lines) phase $[\Phi_{43}(\lambda)]$ and partial phases $[\Phi_{43/1}(\lambda), \Phi_{43/2}(\lambda)]$ for computer generated data.

The resulting minimum mean-squared error is

$$\int |A(\lambda)|^2 [f_{NN}(\lambda) - F_{NM}(\lambda) F_{MM}^{-1}(\lambda) F_{MN}(\lambda)] \, d\lambda \tag{7.3a}$$

or

$$\int |A(\lambda)|^2 [1 - |R_{N \cdot M}(\lambda)|^2] f_{NN}(\lambda) \tag{7.3b}$$

where

$$|R_{N \cdot M}(\lambda)|^2 = \frac{F_{NM}(\lambda) F_{MM}^{-1}(\lambda) F_{MN}(\lambda)}{f_{NN}(\lambda)} \tag{7.4}$$

is called the multiple coherence at frequency λ of the N-process with the processes $M_1, \ldots, M_r$.

The multiple coherence of order-k may be written in terms of ordinary coherences and lower order partial coherences as

$$\begin{aligned} |R_{N \cdot M}|^2 = {} & |R_{NM_1}|^2 + |R_{NM_2/M_1}|^2 [1 - |R_{NM_1}|^2] + \\ & |R_{NM_3/M_1M_2}|^2 [1 - |R_{NM_1}|^2] [1 - |R_{NM_2/M_1}|^2] + \cdots + \\ & |R_{NM_r/M_1 \ldots M_{r-1}}|^2 [1 - |R_{NM_1}|^2] [1 - |R_{NM_2/M_1}|^2] \ldots [1 - |R_{NM_{r-1}/M_1 \ldots M_{r-2}}|^2] \end{aligned} \tag{7.5}$$

suppressing the dependencies on λ.

The partial coherences themselves may be expressed in terms of lower order coherences, suppressing the dependencies on λ, as

$$|R_{NM_r/M_1 \ldots M_{r-1}}|^2 = \frac{|R_{NM_r/M_1 \ldots M_{r-2}} - R_{NM_{r-1}/M_1 \ldots M_{r-2}} R_{M_{r-1}M_r/M_1 \ldots M_{r-2}}|^2}{[1 - |R_{NM_{r-1}/M_1 \ldots M_{r-2}}|^2] [1 - |R_{M_{r-1}M_r/M_1 \ldots M_{r-2}}|^2]}. \tag{7.6}$$

The Fourier transforms of $a(\cdot)$, $b_1(\cdot)$, $b_2(\cdot), \ldots, b_r(\cdot)$, denoted as $A(\lambda)$, $B_1(\lambda)$, $B_2(\lambda), \ldots, B_r(\lambda)$, respectively, satisfy the normal equation

$$B_{NM}(\lambda) F_{MM}(\lambda) = A(\lambda) F'_{NM}(\lambda) \tag{7.7}$$

where

$$B_{NM}(\lambda) = [B_1(\lambda), B_2(\lambda), \ldots, B_r(\lambda)] \tag{7.8}$$

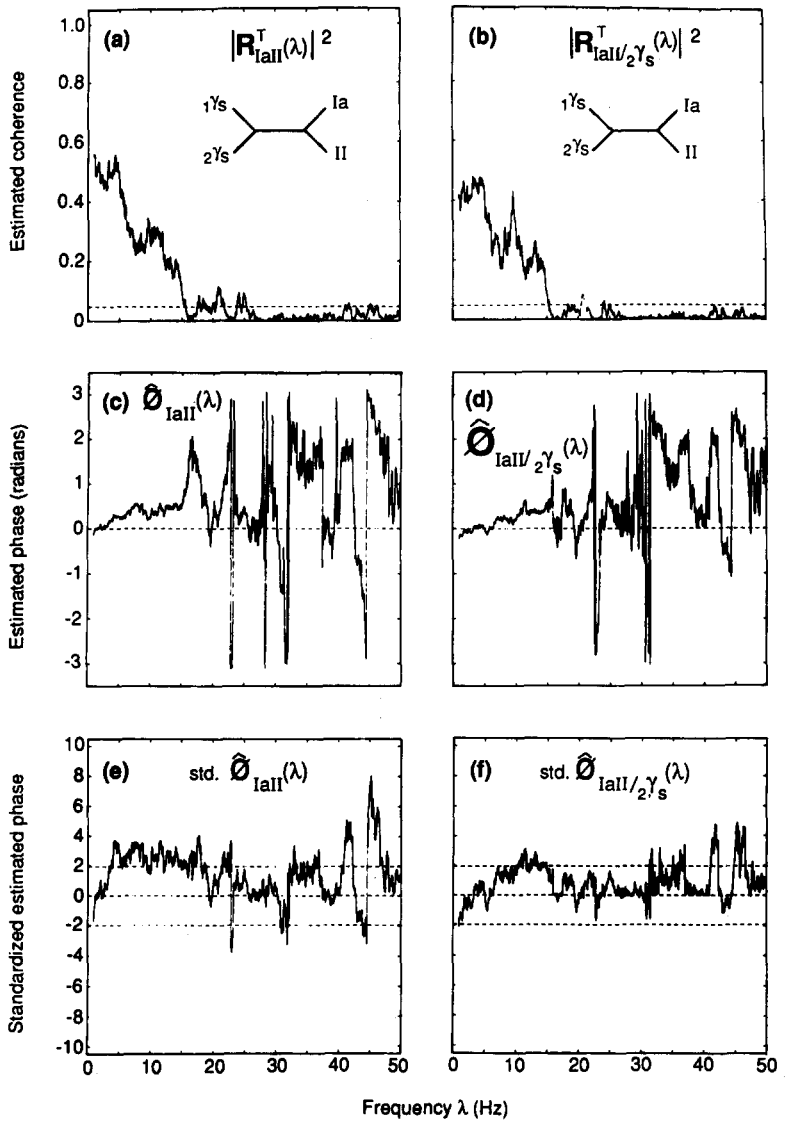

FIG. 12. A comparison of (a) the coherence and (b) the phase of the response of Ia and II sensory endings from the same muscle spindle during independent stimulation of two static fusimotor axons with the (c) partial coherence and (d) partial phase taking into account the contribution of the activity of one of the fusimotor axons. (e, f) Graphical representation of the test for zero phase in (a) and (b), respectively. Points lying outside the the horizontal dashed lines in (e, f), indicating an approximate 95% confidence interval, indicate frequencies where the phase difference is likely to be non-zero. The horizontal dashed lines in (a, b) represent the upper level of an approximate 95% confidence interval for the coherence for any specific value of the frequency λ under the hypothesis that the two processes are independent.

and $F'_{NM}(\lambda)$ is the transpose of $F_{NM}(\lambda)$,

$$F_{MM}(\lambda)=\begin{bmatrix} f_{M_1M_1}(\lambda) & \cdots & f_{M_1M_r}(\lambda) \\ \vdots & & \\ f_{M_rM_1}(\lambda) & \cdots & f_{M_rM_r}(\lambda) \end{bmatrix} \tag{7.9}$$

and

$$F'_{NM}(\lambda)=[f_{NM_1}(\lambda), f_{NM_2}(\lambda), \ldots, f_{NM_r}(\lambda)]. \tag{7.10}$$

Expression (7.7) may also be written as

$$B_{NM}(\lambda) = A(\lambda)F'_{NM}(\lambda)F^{-1}_{MM}(\lambda). \tag{7.11}$$

These results simply extend the results presented earlier and may be further generalized to a pair of vector processes as follows.

Let $[N(t), M(t)]$ denote a stationary bivariate point process, where $N(t)$ and $M(t)$ are respectively s- and r-vector valued processes.

Consider the problem of predicting the vector of values

$$\begin{bmatrix} \int a_1(t)\,\mathrm{d}N_1(t) \\ \vdots \\ \int a_s(t)\,\mathrm{d}N_s(t) \end{bmatrix} \tag{7.12}$$

from

$$\begin{bmatrix} \int b_1(s)\,\mathrm{d}M_1(s) \\ \vdots \\ \int b_r(s)\,\mathrm{d}M_r(s) \end{bmatrix}. \tag{7.13}$$

Let

$$A(\lambda) = \begin{bmatrix} A_1(\lambda) \\ \vdots \\ A_s(\lambda) \end{bmatrix} = \begin{bmatrix} \int \mathrm{e}^{-i\lambda t}a_1(t)\mathrm{d}t \\ \vdots \\ \int \mathrm{e}^{-i\lambda t}a_s(t)\mathrm{d}t \end{bmatrix}. \tag{7.14}$$

The minimum mean-squared error achieved is

$$\int \overline{A(\lambda)}A'(\lambda) * [F_{NN}(\lambda) - F_{NM}(\lambda)F^{-1}_{MM}(\lambda)F_{MN}(\lambda)]\,\mathrm{d}\lambda \tag{7.15}$$

where "$*$" denotes Hadamard product. Expression (7.15) may also be written as

$$\int \overline{A(\lambda)}A'(\lambda) * \{F^{1/2}_{NN}(\lambda)[I - F^{-1/2}_{NN}(\lambda)F_{NM}(\lambda)F^{-1}_{MM}(\lambda)F_{MN}(\lambda)F^{-1/2}_{NN}(\lambda)]F^{1/2}_{NN}(\lambda)\}\,\mathrm{d}\lambda \tag{7.16}$$

where

$$F^{-1/2}_{NN}(\lambda)F_{NM}(\lambda)F^{-1}_{MM}(\lambda)F_{MN}(\lambda)F^{-1/2}_{NN}(\lambda) \tag{7.17}$$

may be thought of as the generalized multiple coherence between vector-valued processes $N(t)$ and $M(t)$.

Further, the elements of the matrix

$$F_{NN}(\lambda) - F_{NM}(\lambda)F^{-1}_{MM}F_{MN}(\lambda) \tag{7.18}$$

from expression (7.15) are defined as the partial spectra between components of $N(t)$ after removing the contribution of $M(t)$. The elements of (7.18) may be denoted as $f_{N_iN_j/M}(\lambda)$ where $i=j$ gives the partial auto-spectra and $i \neq j$ the partial cross-spectra of the components N_i, N_j of $N(t)$ after removing the contribution of $M(t)$.

The partial coherence between the i^{th} and j^{th} components of $N(t)$ after removing the contribution from $M(t)$ may be written in terms of the partial spectra as

$$|R_{N_iN_j/M}(\lambda)|^2 = \frac{|f_{N_iN_j/M}(\lambda)|^2}{F_{N_iN_i/M}(\lambda)f_{N_jN_j/M}(\lambda)}. \tag{7.19}$$

The partial phase is written in terms of the entries of (7.18) as

$$\Phi_{N_iN_j/M}(\lambda) = \arg\{f_{N_iN_j/M}(\lambda)\}. \tag{7.20}$$

Expressions (7.18)–(7.20) may also be evaluated for $k \leq r$ to obtain partial spectra, partial coherences and partial phases of order-k, for k components of $M(t)$, by making the appropriate changes to $F_{NM}(\lambda)$, F_{MM} and $F_{MN}(\lambda)$. Once the basic auto- and cross-spectra have been computed all the coherences and coherence-related parameters of all orders may be found by simple algebraic combinations of these spectra.

VIII. EXAMPLES OF PARTIAL COHERENCE AND PARTIAL PHASE (ORDER-1, 2)

The examples of this section describe further applications of partial coherence and partial phase of order-1 followed by their extensions to order-2, first to simulated data to allow a comparison between derived and estimated parameter values for processes that are simply related, and then to real data on muscle spindles where several inputs are under independent experimental control.

The simulated data-set given in this section extends the example of partial coherence (Fig. 8) and of partial phase (Fig. 11) for the simulated data of Section VI to the case where one can examine how more than one spike train can influence both the strength of association and timing between two other trains. This example approaches more closely to real conditions where several spike trains from different sources act simultaneously on a group of neurones (e.g. Baldissera *et al.*, 1981).

The simulated data-set is constructed as follows. Let I, II, III, ε_1, and ε_2 represent five independent stochastic point processes with σ_{ij} the time of occurrence of the j^{th} event of the i^{th} process for $i=1,2,\ldots,5$ and $j=1,2,\ldots$. These five processes are arranged according to the scheme set out below to form four processes which are assumed to be the observable processes. In the superimposed processes the I, II, III, ε_1, and ε_2 components are not separately observable, i.e., particular spike times cannot be associated with particular component processes. The observable processes are taken to be

$$N_1(t)=\mathrm{I}$$

$$N_2(t)=\mathrm{II}$$

$$N_3(t)=\mathrm{I}+\mathrm{II}+\mathrm{III}+\varepsilon_1$$

$$N_4(t)=(\mathrm{I}+d_1)+(\mathrm{II}+d_2)+(\mathrm{III}+d_3)+\varepsilon_2$$

where d_1, d_2 and d_3 are fixed time delays. Consider the problem of estimating the strength of association and the phase between processes $N_3(t)$ and $N_4(t)$ when the contributions from processes $N_1(t)$ and $N_2(t)$ are taken into account first separately and then together. The analytic solution to this problem depends on the computation of a number of point-process spectra, and is a direct application of the expressions set out in Sections III, V and VII.

The observed coherences and phases for the simulated data take on particularly clear and easily interpretable forms if the processes I, II and III are chosen to be independent Poisson processes with the same mean intensities, and the delays, d_1, d_2 and d_3 are equally spaced, as well as small to avoid the biases that can occur in naive phase estimates for long delays (Brillinger and Tukey, 1984). Under these assumptions the derived parameters have particularly simple forms. The derived phase, for example, is

$$\Phi_{43}(\lambda)=-\left(\frac{d_1+d_2+d_3}{3}\right)\lambda \tag{8.1}$$

and the derived partial phases are

$$\Phi_{43/1}(\lambda)=-\left(\frac{d_2+d_3}{2}\right)\lambda \tag{8.2}$$

$$\Phi_{43/2}(\lambda)=-\left(\frac{d_1+d_3}{2}\right)\lambda \tag{8.3}$$

and

$$\Phi_{43/12}(\lambda)=-d_3\lambda. \tag{8.4}$$

This special case is not only instructive in illustrating the usefulness of partial coherence and partial phase, but actually occurs in a number of real data cases where delays predominate and the input processes can be chosen to be realizations of Poisson processes (Halliday *et al.*, 1988).

The estimated coherences and phases in the following examples are based entirely on the auto- and cross-spectra of the sets of spike times for the observable processes $N_1(t)$, $N_2(t)$, $N_3(t)$ and $N_4(t)$. The derived curves follow from the application of the appropriate expressions given in Sections III, V and VII. The derived and estimated coherence and phase between $N_3(t)$ and $N_4(t)$, in the presence of the observable processes $N_1(t)$ and $N_2(t)$, are shown plotted on the same graph (Fig. 13a, b), and clearly illustrate the close agreement between derived and estimated values for both. In the presence of both $N_1(t)$ and $N_2(t)$ the coherence remains significant to approximately 65 Hz decreasing slowly from a peak value of approximately 0.52, while the linear phase curve indicates a system dominated by a delay of approximately 2 msec, with process $N_4(t)$ leading process $N_3(t)$.

If one takes into account the contribution of process $N_1(t)$ to the coherence and phase between $N_3(t)$ and $N_4(t)$, illustrated in Fig. 13c, d, the peak value of the coherence is now about 0.4, but remains significant to about 100 Hz, in contrast to the ordinary coherence which was significant only to approximately 65 Hz. The change in phase is dramatic (Fig. 13d compared with Fig. 13b). Removing the linear contribution of process $N_1(t)$ suggests that process $N_2(t)$ alone synchronizes processes $N_3(t)$ and $N_4(t)$, whereas the main contribution of process $N_1(t)$ is to induce a phase shift between $N_3(t)$ and $N_4(t)$.

Taking into account the linear contribution of $N_2(t)$ to the coherence between $N_3(t)$ and $N_4(t)$ produces quite different consequences.

The partial phase (Fig. 13f) remains the same as the original phase (Fig. 13b), whereas the partial coherence (Fig. 13e) becomes strikingly periodic, although it does not reach the same peak value as the ordinary coherence (Fig. 13a). These results suggest that when both processes $N_1(t)$ and $N_2(t)$ are present, process $N_1(t)$ has a predominant effect on the coherence between $N_3(t)$ and $N_4(t)$, whereas $N_2(t)$ primarily affects the timing between $N_3(t)$ and $N_4(t)$. It is far from clear how one could be led to such conclusions by time-domain analyses.

The second-order partial coherence (Fig. 13g) is small but significant, whereas the second-order partial phase (Fig. 13h) indicates a phase lag of $N_4(t)$ with respect to $N_3(t)$. These two measures taken together suggest the presence of another source of coupling. This situation is most likely to occur when recording several processes simultaneously within the central nervous system. The phase dependence of output processes on input conditions was demonstrated for muscle spindle data in Section VI.

Figure 14 is an illustration of the application of the second-order partial coherence to the responses of the Ia and II sensory endings from the same muscle spindle in the presence of an imposed dynamic length change with concurrent independent stimulation of two static fusimotor axons. The ordinary coherence (Fig. 14a) shows two distinct regions of coupling between the responses of the Ia and II endings in the presence of the three inputs. The first region covers the frequency range from 0 up to 17 Hz, whereas the second region occupies the range from about 30–60 Hz. The second-order partial coherence taking into account the contribution of the activity of the two static fusimotor axons shows a significant reduction of the coherence in the low frequency range alone—the coherence in the higher range remains unchanged (Fig. 14b). This result suggests that the coupling in the 30–60 Hz range is entirely length dependent, whereas that in the lower range is not entirely accounted for by the linear contribution from the fusimotor input and, in addition, there may be a length contribution to the low-frequency coupling. The former supposition may be examined by considering a more complicated contribution of the fusimotor input to the Ia–II coupling than that provided by the linear prediction of the contribution of the fusimotor input as well as taking into account the contribution of the length input to the coherence at low frequencies.

IX. CONCLUDING REMARKS

We have extended, particularized and elaborated the applications of Fourier methods to the analysis of the interactions between spike trains by considering a broader range of questions than discussed by previous authors (e.g. Stein *et al.*, 1972), and by drawing upon many examples from both simulated and real data. Throughout the presentation we have implicitly stressed the necessity for having approximations to the statistical uncertainty of all

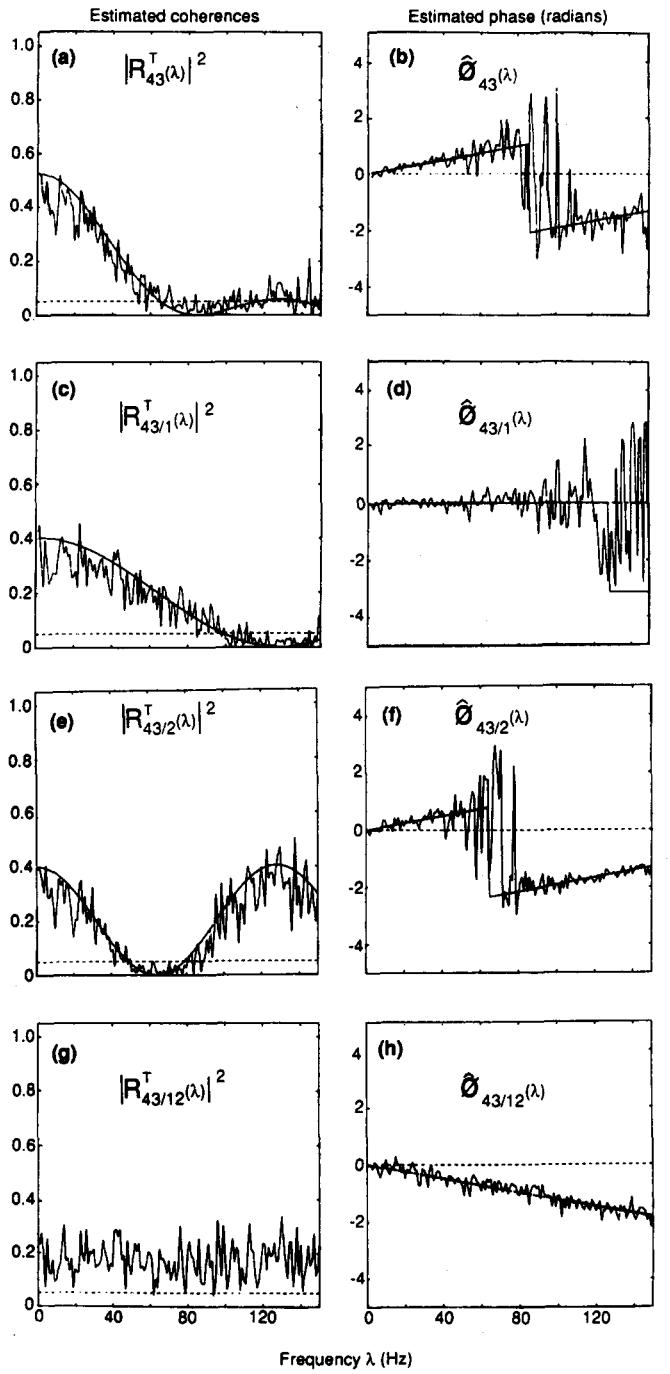

FIG. 13. Derived (unbroken curves) and estimated (a) coherence, (b) phase between computer generated processes N_3 and N_4, (c, d) partial coherences, (e, f) partial phases of order-1, (g) partial coherence and (h) partial phase of order-2 between computer generated processes N_3 and N_4 taking into account the effects of processes N_1 and N_2 separately and together. The horizontal dashed line in the coherence plots represents the upper level of an approximate 95% confidence interval for the coherence for any specific value of the frequency λ under the hypothesis that the two processes are independent.

the estimates of the parameters defined and applied to the various data sets. The approximate sampling fluctuations of the data-based estimates allow one to set up statistical tests and to make inferences concerning the population parameters.

In this paper we have dealt with two main issues: (1) the importance of alternative representations of the data, and (2) the use of Fourier-based measures that give rise to

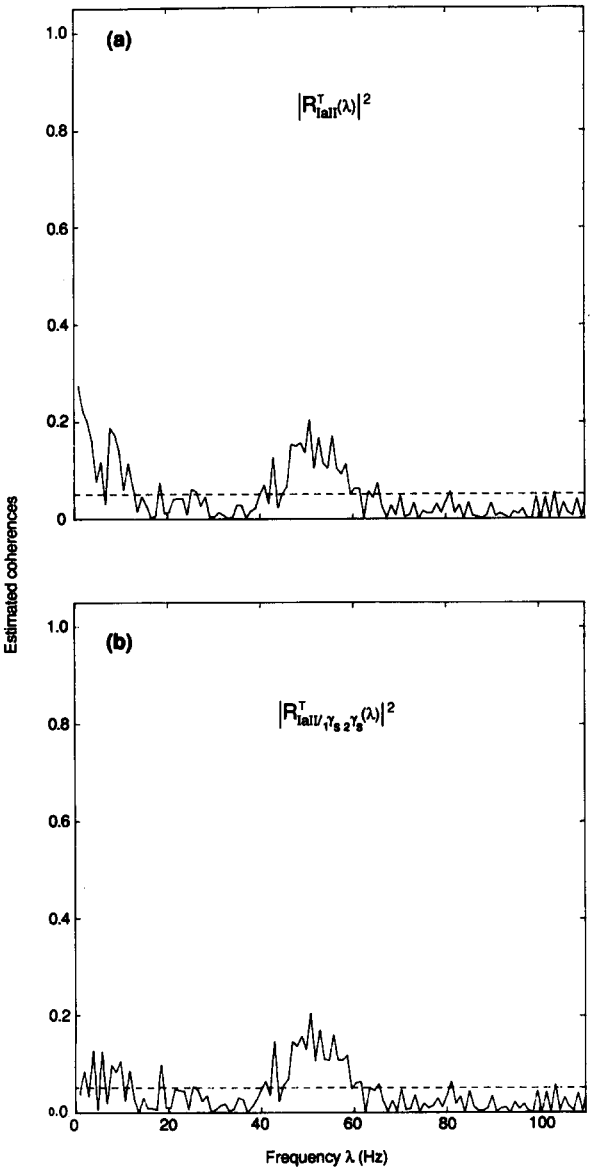

FIG. 14. (a) Coherence between the responses of Ia and II sensory endings from the same muscle spindle in response to independent stimulation of two fusimotor axons during a random length change applied to the parent muscle. (b) Partial coherence of order-2 between the responses of the Ia and II endings taking into account the linear contribution from both static fusimotor axons. The horizontal dashed lines represent the upper level of an approximate 95% confidence interval for the coherence for any specific value of the frequency λ under the hypothesis that the two processes are independent.

techniques for analysing neuronal interactions that are not available within a cross-intensity based framework. Our concluding remarks relate to these two issues.

It is sometimes assumed that time- and frequency-domain methods give equivalent representations of a data set, because they are mathematically equivalent and both contain the same information about the processes involved; and consequently, it is sufficient to use only one of these representations (Tukey, 1978; Koopmans, 1983). A further example to those presented in Section IV forcefully illustrates again that because of the finite amount of data mathematical equivalence does not imply equivalent representation (Tukey, 1978). The curves shown as solid lines in Fig. 15a, c, e are the estimated auto-intensities of the Ia responses from a muscle spindle under three different input conditions imposed on the spindle. These auto-intensities were computed directly from the times of occurrence of the

spikes of the Ia discharge. The shapes of the auto-intensities do not differ greatly, although in Fig. 14a the spindle was subjected to a randomly varying fusimotor input, whereas in Fig. 15c a random length change was imposed on the parent muscle, and in Fig. 15e both of these inputs were applied simultaneously.

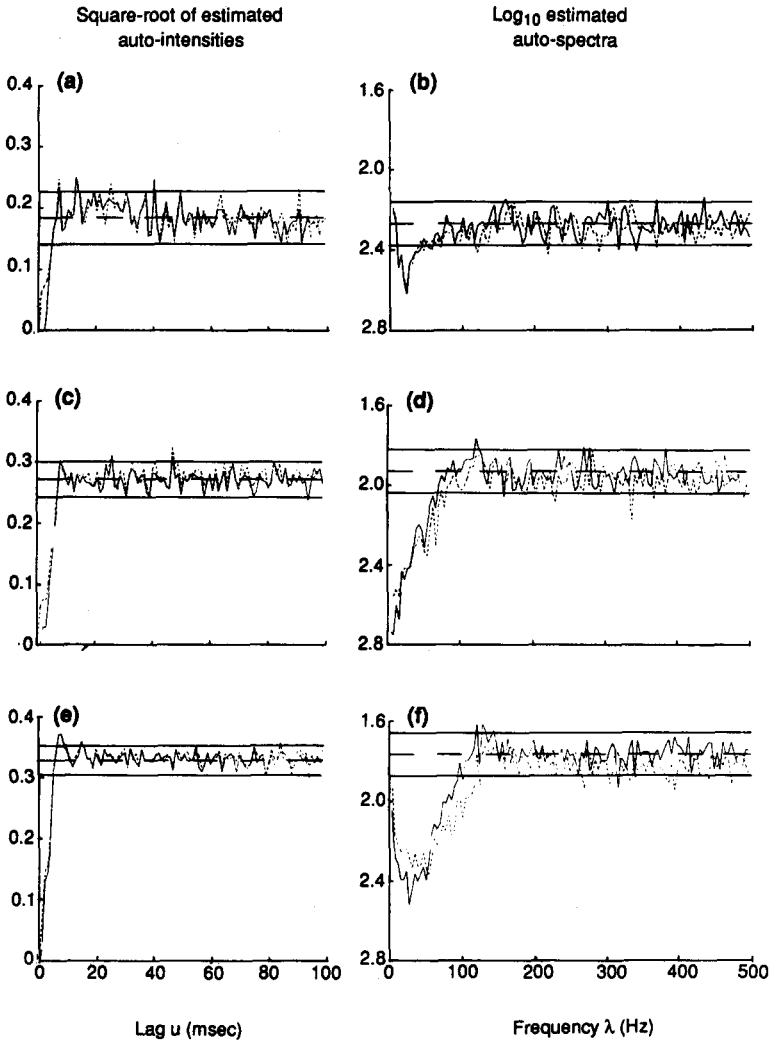

FIG. 15. (a, c, e) The square-root of the estimated auto-intensity functions computed directly from the times of occurrence of the Ia spikes (solid lines) and from the Fourier transforms of the auto-spectra (dashed lines). (b, d, f) The estimated auto-spectra computed directly from the Ia spike times (solid lines) and from the Fourier transform of the auto-intensity function (dashed lines), during (a, b) random stimulation of a single static fusimotor axon, (c, d) in the presence of a randomly varying length change, and (e, f) with both fusimotor and length inputs present. The solid horizontal lines in (a, c, e) give an approximate 95% confidence interval for the auto-intensity function for any specific value of the lag u. The solid horizontal lines in (b, d, f) are an approximate 95% confidence interval for the auto-spectra for any specific value of the frequency λ.

Under these different input conditions one would expect the auto-intensities to be quite different. The right-hand column of Fig. 15 represents the auto-spectra of the Ia discharge, also computed directly from the times of occurrences of the Ia spikes, for the same three input conditions. The shape of the auto-spectra are quite different for each of the different input conditions. The differences in shape of the auto-spectra in Fig. 15b, d, f led to the suggestion that, under certain conditions, the spectrum of the Ia discharge when both length and fusimotor inputs are present simultaneously is a linear combination of the effects produced by each input alone (Rosenberg and Rigas, 1985). That the representations of the data in Fig. 15a, c, e are mathematically equivalent to those in Fig. 15b, d, f is demonstrated

by the dotted lines, which in Fig. 15a, c, e are the Fourier transforms of the corresponding member of the pair in Fig. 15b, d, f. In addition, the dotted lines in Fig. 15b, d, f are the Fourier transforms of the corresponding member of the pair in Fig. 15a, c, e. The extremely close fit between the measure computed directly from the data with that derived from the Fourier transform of either the auto-intensity or the auto-spectrum indicates the mathematical equivalence of these different representations. The striking differences between the appearance of the representations of the data illustrates that mathematical equivalence does not always lead to equivalent emphasis of distinctive features of the data. In this example the Fourier representation of the data happens to be more useful. In general, it seems that one should use both time- and frequency-domain representations, particularly when faced with the problem of revealing the properties of complex systems (Tukey, 1978).

It is of interest to note that both the framework for multiple spike train analysis proposed by Gerstein *et al.* (1985) and Gerstein and Aertsen (1985), and the Fourier-based methods presented in this paper lead to analyses within the standard mathematical statistical framework of multivariate analysis. The former may use cluster analysis to examine the dynamic evolution of neural assemblies along the lines suggested by Wright (1977), whereas the latter draws mainly upon regression analysis.

In conclusion, frequency-domain analyses based on coherence measures considerably extend the range of tools available for the analysis of spike trains and can lead to new insight and understanding of the interactions between spike trains.

ACKNOWLEDGEMENTS

This work was supported in part by a grant from the Medical Research Council of Great Britain to J.R. D.R.B.'s research is supported in part by National Science Foundation Grant DMS-36884. A.M.A. is supported by a grant from the Federal Government of Pakistan and the Provincial Government of Baluchistan, Pakistan. D.M.H. is supported by the Wellcome Trust.

REFERENCES

AMJAD, A. M., BREEZE, P., CONWAY, B. A., HALLIDAY, D. M. and ROSENBERG, J. R. (1988) A framework for the analysis of neuronal networks. *Progr. Brain Res.*, in press.

AERTSEN, A. M. H. J. and GERSTEIN, G. L. (1985) Evaluation of neuronal connectivity: sensitivity of cross-correlation. *Brain Res.* **340,** 341–354.

BALDISSERA, F., HULTBORN, H. and ILLERT, M. (1981) Integration in spinal neuronal systems. In *Handbook of Physiology*, Section 1, *The Nervous System*, Vol. II, part 1 *Motor Control.* (ed. V. B. BROOKS), pp. 509–595. American Physiological Society, Bethesda, MD, U.S.A.

BARTLETT, M. S. (1963) The spectral analysis of point processes. *J.R. Stat. Soc.* **B25,** 264–280.

BESSOU, P. and LAPORTE, Y. (1963) Responses from primary and secondary endings of the same neuromuscular spindle of the tenuissimus of the cat. In *Symposium on Muscle Receptors* (ed. D. BARKER), pp. 105–119. Hong Kong University Press, Hong Kong.

BRILLINGER, D. R. (1975a) The identification of point process systems. *Ann. Probab.* **3,** 909–929.

BRILLINGER, D. R. (1975b) *Time Series—Data Analysis and Theory.* Holt, Rinehart & Winston, New York.

BRILLINGER, D. R. (1978) Comparative aspects of the study of ordinary time series and point processes. In *Developments in Statistics*, Vol. 5 (ed. P. R. KRISHNAIAH), pp. 33–133. Academic Press, New York.

BRILLINGER, D. R. (1983) The finite Fourier transform of a stationary process. In *Handbook of Statistics*, Vol. 3 (eds. D. R. BRILLINGER and P. R. KRISHNAIAH), pp. 21–37. Elsevier, Amsterdam.

BRILLINGER, D. R. (1986) Some statistical methods for random process data from seismology and neurophysiology. *Department of Statistics, University of California, Berkeley Technical Report No. 84.* p. 28.

BRILLINGER, D. R. and TUKEY, J. W. (1984) Spectrum analysis in the presence of noise: some issues and examples. In *The Collected Works of J. W. Tukey*, Vol. 3 (ed. D. R. BRILLINGER), pp. 1002–1141.

BRILLINGER, D. R., BRYANT, H. L. JR and SEGUNDO, J. P. (1976) Identification of synaptic interactions. *Biol. Cybern.* **22,** 213–228.

BRYANT, H. L. JR, RUIZ MARCOS, A. and SEGUNDO, J. P. (1973) Correlations of neuronal spike discharges produced by monosynaptic connections and by common inputs. *J. Neurophysiol.* **36,** 205–225.

CHRISTAKOS, C. N., ROST, I. and WINDHORST, U. (1984) The use of frequency domain techniques in the study of signal transmission in skeletal muscle. *Pflügers Arch. ges. Physiol.* **400,** 100–105.

CLARK, F. J., MATTHEWS, P. B. C. and MUIR, R. B. (1981) Response of Ia afferents to vibration in the presence of the tonic vibration reflex. *J. Physiol.* **311,** 97–112.

COX, D. R. and ISHAM, V. (1980) *Point Processes.* Chapman & Hall, London.

COX, D. R. and LEWIS, P. A. W. (1968) *The Statistical Analysis of Series of Events.* Methuen, London.

COX, D. R. and LEWIS, P. A. W. (1972) Multiple Point Processes. In *Proc. 6th Berkeley Symposium Math. Statist. Probab.*, Vol. 3 (eds. L. M. LECAM, J. NEYMAN and E. L. SCOTT), pp. 401–448. University of California Press, Berkeley.

DALEY, D. J. and VERE-JONES, D. (1988) *An Introduction to the Theory of Point Processes.* Springer, New York.

EDGLEY, S. A. and JANKOWSKA, E. (1987) An interneuronal relay for group I and II muscle afferents in the midlumbar segments of cat spinal cord. *J. Physiol.* **389,** 647–674.
ELLAWAY, P. H. and MURTHY, K. S. K. (1985a) The origins and characteristics of cross-correlated activity between γ-motoneurones in the cat. *Q. Jl exp. Physiol.* **70,** 219–232.
ELLAWAY, P. H. and MURTHY, K. S. K. (1985b) The source and distribution of short-term synchrony between γ-motoneurones in the cat. *Q. Jl exp. Physiol.* **70,** 233–247.
GERSTEIN, G. L. and AERTSEN, A. M. H. J. (1985) Representation of cooperative firing among simultaneously recorded neurones. *J. Neurophysiol.* **54,** 1513–1528.
GERSTEIN, G. L. and KIANG, N. Y.-S. (1960) An approach to the quantitative analysis of electrophysiological data from single neurones. *Biophys. J.* **1,** 15–28.
GERSTEIN, G. L., PERKEL, D. H. and DAYHOFF, J. E. (1985) Cooperative firing activity in simultaneously recorded populations of neurones: detection and measurement. *J. Neurosci.* **5,** 881–889.
GRIFFITH, J. S. and HORN, G. (1963) Functional coupling between cells in the visual cortex of the unrestrained cat. *Nature* **199,** 893–895.
HALLIDAY, D. M., GLADDEN, M. H. and ROSENBERG, J. R. (1988) Fusimotor induced phase differences between responses of primary and secondary endings from the same muscle spindle. In *Mechanoreceptors—Development, Structure, Function* (eds. P. HNIK and T. SOUKUP), Plenum, New York, in press.
HOLDEN, A. V. (1976) Models of stochastic activity in neurones. In *Lecture Notes in Biomathematics*, Vol. 12 (ed. S. LEVIN), Springer-Verlag, Berlin.
HOUK, J. C., DESSEM, D. A., MILLER, L. E. and SYBIRSKA, E. H. (1987) Correlation and spectral analysis of relations between single unit discharge and muscle activity. *J. Neurosci. Methods* **21,** 201–224.
JENKINS, G. and WATT, D. G. (1968) *Spectral Analysis and its Applications*. Holden-Day, San Francisco.
KENDALL, M. G. and STUART, A. (1969) *The Advanced Theory of Statistics*, Vol. 2. Griffin, London.
KIRKWOOD, P. A. (1979) On the use and interpretation of cross-correlation measurements in the mammalian central nervous system. *J. Neurosci. Methods* **1,** 107–132.
KIRKWOOD, P. A. and SEARS, T. A. (1980) The measurement of synaptic connections in the mammalian central nervous system by means of spike triggered averaging. In *Prog. in Clin. Neurophysiol.*, Vol. 8 (ed. J. E. DESMEDT), pp. 44–71. Karger, Basel.
KIRKWOOD, P. A. and SEARS, T. A. (1982) The effect of single afferent impulses on the probability of firing of external intercostal motoneurones in the cat. *J. Physiol.* **322,** 315–336.
KOOPMANS, L. H. (1983) A spectral analysis primer. In *Handbook of Statistics*, Vol. 3 (eds. D. R. BRILLINGER and P. R. KRISHNAIAH), pp. 169–184. Elsevier, Amsterdam.
LEWIS, P. A. W. (1972a) Remarks on the theory, computation, and application of the spectral analysis of series of events. *J. Sound and Vib.* **12,** 353–375.
LEWIS, P. A. W. (ed.) (1972b) *Stochastic Point Processes*. John Wiley, New York.
MATTHEWS, P. B. C. (1981) Review Lecture: Evolving views on the internal operation and functional role of the muscle spindle. *J. Physiol.* **320,** 1–30.
MELSSEN, W. J. and EPPING, W. J. M. (1987) Detection and estimation of neural connectivity based on cross-correlation analysis. *Biol. Cybern.* **57,** 403–414.
MOORE, G. P., PERKEL, D. H. and SEGUNDO, J. P. (1966) Statistical analysis and functional interpretation of neuronal spike data. *A. Rev. Physiol.* **28,** 493–552.
PERKEL, D. H., GERSTEIN, G. L. and MOORE, G. P. (1967a) Neuronal spike trains and stochastic point processes. I. The single spike train. *Biophys. J.* **7,** 391–418.
PERKEL, D. H., GERSTEIN, G. L. and MOORE, G. P. (1967b) Neuronal spike trains and stochastic point processes. II. Simultaneous spike trains. *Biophys. J.* **7,** 419–440.
ROSENBERG, J. R. and RIGAS, A. (1985) Spectral composition of muscle spindle Ia responses to combined length and fusimotor inputs. In *The Muscle Spindle* (eds. I. A. BOYD and M. H. GLADDEN), pp. 397–402. Macmillian, London.
SEARS, T. A. and STAGG, D. (1976) Short term synchronization of intercostal motoneurone activity. *J. Physiol.* **263,** 357–387.
STEIN, R. B., FRENCH, A. S. and HOLDEN, A. V (1972) The frequency response, coherence and information capacity of two neuronal models. *Biophys. J.* **12,** 295–322.
TICK, L. J. (1963) Conditional spectra, linear systems, and coherency. In *Time Series Analysis* (ed. M. ROSENBLATT), pp. 197–203. Wiley, New York.
TORRES-MELO, L. (1974) *Stationary Point Processes*. Ph.D. Thesis University of California, Berkeley.
TOYAMA, K., KIMURA, M. and TANAKA, K. (1981) Cross-correlation analysis of interneuronal connectivity in cat visual cortex. *J. Neurophysiol.* **46,** 191–201.
TUKEY, J. W. (1978) Can we predict where time series should go next? In *Institute of Mathematical Statistics—Reports on Directions in Time Series* (eds. D. R. BRILLINGER and G. C. TIAO), pp. 1–31. Iowa State University, Ames.
WIENER, N. (1930) Generalised harmonic analysis. *Acta math.* **55,** 117–258.
WEISBERG, S. (1985) *Applied Linear Regression*. 2nd edn. John Wiley, New York.
WONNACOTT, D. H. and WONNACOTT, R. J. (1981) *Regression: A Second Course in Statistics*.
WRIGHT, W. E. (1977) Gravitational clustering. *Pat. Recogn.* **9,** 151–166.

APPENDIX

In neural systems whose dynamics are dominated by delays, the phase relation between input and output spike trains, $\Phi(\lambda)$, is given as

$$\Phi(\lambda) = -\tau\lambda \tag{10.1}$$

where τ is the time delay between these processes. The delay may be estimated as the slope of

the least squares line fitted to the estimated phase curve. In most cases, however, the coherence between input and output processes is not constant, and consequently a weighted least squares procedure must be used to estimate the delay and its standard error.

If we let $\Phi^T(\lambda_i) \equiv \Phi_i$ represent the estimated phase defined at $\lambda_i = 2\pi i/T, i = 1, 2, \ldots, n$, then a regression model through the origin of the following form may be set down

$$\Phi_i = \beta\lambda_i + \varepsilon_i \tag{10.2}$$

where $\beta = -\tau$, and the ε_i are approximately normally distributed with mean zero and variance σ_i^2, and covariance

$$\text{cov}\{\varepsilon_i, \varepsilon_j\} \cong 0 \text{ for } i \neq j. \tag{10.3}$$

From Section III we have that the variance σ_i^2 is

$$\sigma_i^2 = \frac{1}{2L}\left[\frac{1}{|R_1(\lambda_i)|^2} - 1\right] \tag{10.4}$$

where L is the number of disjoint periodogram sections from records of duration T used in estimating the spectra required to estimate $\Phi(\lambda)$.

The non-constant variance given by expression (10.4) suggests a weighted least squares estimate of β, that may be obtained by minimizing

$$\sum \frac{1}{\sigma_i^2}(\Phi_i - \beta\lambda_i)^2 \tag{10.5}$$

(e.g. Wonnacott and Wonnacott, 1981).
If we set

$$\sigma_i^2 = \frac{\sigma^2}{w_i^2} \tag{10.6}$$

where w_i is the weight for the i^{th} value of the variance, then the weighted least squares estimate of β is given by

$$\hat{\beta} = \frac{\sum w_i \Phi_i \lambda_i}{\sum w_i \lambda_i^2}. \tag{10.7}$$

Expression (10.7) is an unbiased estimate of β, and is approximately normally distributed with variance

$$\text{Var}(\hat{\beta}) = \frac{\sigma_2}{\sum w_i \lambda_i^2}. \tag{10.8}$$

An obvious estimate of σ^2 is given by

$$\hat{\sigma}^2 = \frac{\sum w_i(\Phi_i - \hat{\beta}\lambda_i)^2}{n-1}. \tag{10.9}$$

A simple but plausible and common choice for the weights is to take the w_i as inversely proportional to the estimated variance given by

$$w_i \propto \frac{1}{\hat{\sigma}_i^2} \tag{10.10}$$

(e.g. Weisberg, 1985).
An approximate 95% confidence interval for the delay is then

$$-\hat{\beta} \pm t_{(n-1,0.975)} \frac{\hat{\sigma}}{\sqrt{\sum w_i \lambda_i^2}} \tag{10.11}$$

where σ is given by (10.9).